



TOPICAL REVIEW • **OPEN ACCESS**

Recent trends in nanothermites: Fabrication, characteristics and applications

To cite this article: Shruti Kabra *et al* 2020 *Nano Ex.* 1 032001

View the [article online](#) for updates and enhancements.

You may also like

- [From nanoparticles to on-chip 3D nanothermite: electrospray deposition of reactive Al/CuO@NC onto semiconductor bridge and its application for rapid ignition](#)
Ji Dai, Chengai Wang, Yueting Wang et al.
- [Damage aftereffect of energetic materials in armor piercing incendiary projectiles on diesel fuel tanks](#)
K Liu, G T Liu, P G Luo et al.
- [A diagnostic for quantifying heat flux from a thermite spray](#)
E P Nixon, M L Pantoya, D J Prentice et al.





The Electrochemical Society

Advancing solid state & electrochemical science & technology

DISCOVER

how sustainability intersects with electrochemistry & solid state science research







TOPICAL REVIEW

OPEN ACCESS

RECEIVED
2 July 2020REVISED
16 September 2020ACCEPTED FOR PUBLICATION
30 September 2020PUBLISHED
12 October 2020

Original content from this work may be used under the terms of the [Creative Commons Attribution 4.0 licence](#).

Any further distribution of this work must maintain attribution to the author(s) and the title of the work, journal citation and DOI.



Recent trends in nanothermites: Fabrication, characteristics and applications

Shruti Kabra¹, Swaroop Gharde¹, Prakash M Gore¹, Sunil Jain², Vrushali H Khire² and Balasubramanian Kandasubramanian¹

¹ Nano Surface Texturing Laboratory, Department of Metallurgical and Materials Engineering, Defence Institute of Advanced Technology (DU), Ministry of Defence, Girinagar, Pune- 411025, Maharashtra, India

² High Energy Materials Research Laboratory, DRDO, Ministry of Defence, Pune - 411021, Maharashtra, India

E-mail: meetkbs@gmail.com

Keywords: nano energetic materials, aerospace, propulsion, explosive, thermite

Abstract

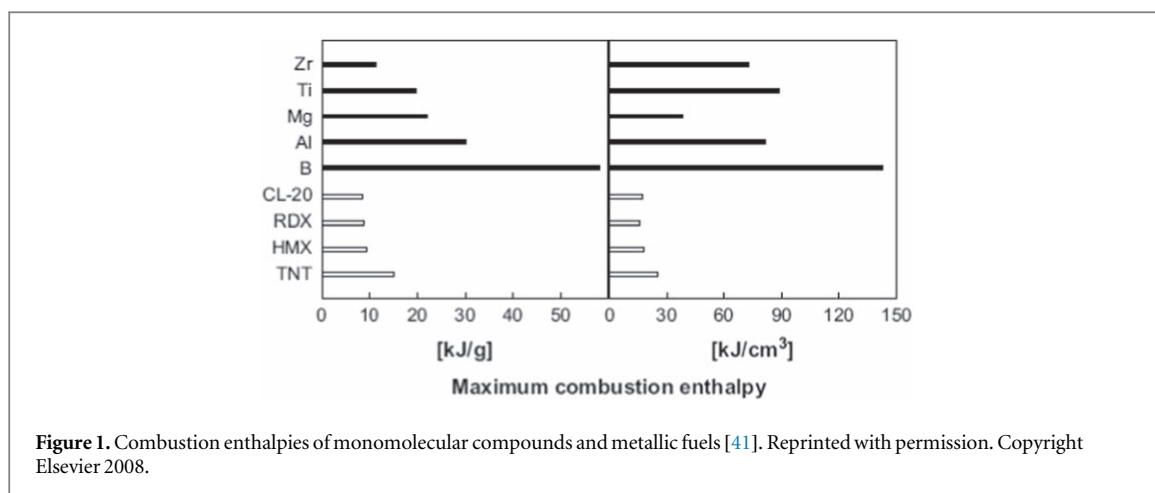
Energetic materials (EMs) are a group of distinctive materials that release an enormous amount of amassed chemical energy in a short time when incited by external mechanical or thermal factors. They comprise of propellants, explosives, and pyrotechnics. Unlike conventional micro-energetic materials, nano energetic materials (nEMs), due to their smaller particle size ranging from 1–100 nm, exhibit higher specific surface area ($\sim 10\text{--}50\text{ m}^2\text{ g}^{-1}$), reduced ignition temperatures from 2350 K to approx. 1000 K for particle size from 100 μm to 100 nm respectively, higher energy densities (up to 50 MJ kg⁻¹), burning rates $\sim 30.48\text{ mm s}^{-1}$ at 6.894 kPa with specific impulses up to 542 s (5320 m s⁻¹), low impact sensitivity ($< 4\text{--}35\text{ J}$). Such exceptional properties of nano energetic composites, i.e., thermites (a combination of metal-fuel/metal oxide particles), find applications, namely in, munitions, pyrotechnics, energetic micro-electromechanical system (MEMS) chips. This review provides valuable insight into the synthesis methods of nano energetic composite systems (e.g., Al/CuO, Al/KMnO₄, Al/Fe₂O₃, Al/SnO₂, Silicon-based systems), their characteristic properties, behavior under certain conditions and applications. Furthermore, the review converses about the advancements made in the last few decades by many researchers, along with the technological gaps that need to be addressed for futuristic applications.

1. Introduction

Energetic Materials cataloged as Propellants, Pyrotechnics, and Explosives [1, 2] are materials that are capable of providing a large quantity of energy by releasing their stored chemical energy when instigated by external factors like impact, friction or shock.

Historically, humans got familiarized with the energetic materials in 220 BC when few Chinese alchemists faced an accidental explosion due to the unintentional production of black powder, also known as Gun powder. Using Roger Bacon's experimental details from 13th century as a reference, Berthold Schwartz further validated the composition of black powder and also scrutinized its properties [3]. By the beginning of the 17th century, the Gun powder was used in detonating mines but had the risk of mine explosions. The need to develop more benign substitute explosive materials led to the discovery of nitroglycerine (NG) and dynamite in the 19th century followed by the development of nitrocellulose (NC), trinitrotoluene (TNT) in the 20th century and various energetic organic nitrate/nitramine compounds like cyclotrimethylene trinitramine (RDX), cyclotetramethylene tetranitramine (HMX), triaminotrinitrobenzene (TATB), in the later years [4–6]. Though energetic materials have been around for a while, the continuous need for enhanced, efficient, safe, and secure energetic materials drives researchers to keep on exploring the world of energetic materials and advance from the conventional energetic compounds to advanced EMs.

Many researchers contributed to understanding the molecular structure [7], the chemical reactions [8], the physicomechanical [9], and optical properties [10], the hazards associated with EMs [11], and the development



of modern energetic materials. Owing to the limited energy densities (ex. 2094 J g^{-1} for TNT) of conventional EMs [12], researchers moved towards the usage of high energy density materials (approx. 30 kJ g^{-1}), i.e., metals as fuels in the synthesis of EMs. With the advent of nanotechnology, nanoparticles of the order of 100 nm or less, because of their exceptional property of high specific surface area, replaced the micron-sized metal particles, thus leading to the fabrication of nanothermites (a mixture of fuel and oxidizers with particle size ranging in nanometric scale), a new realm of nano energetic materials [13]. Building upon the foundation led by the researchers several decades ago, the transition from conventional energetic compounds to advanced nanoenergetic materials took place.

Last two decades have witnessed a remarkable development in the domain of energetic materials. There has been a gradual shift from the usage of nitrocarbon energetic materials such as TNT, RDX, CL-20 to microstructured composites to nanothermites. This paper starts by giving a holistic view of the classification of EMs and then introducing the nanothermites and elaborates the trends in the fabrication methods involved in processing of nanothermites as well as it emphasizes mainly on the most commonly used Al-based nanothermites and their exceptional properties that render them suitable for miscellaneous applications in military, aerospace and civilian sector. Furthermore, it addresses the challenges that need to be resolved in pursuit of the enhanced NEMs for future development.

2. Classification of energetic materials

2.1. Monomolecular energetic materials

Monomolecular EMs, also known as Explosives or Homogeneous reactive materials [14], is a single molecular fusion of fuel and oxidizer constituents. NG [5], TNT [6], NC [15], HMX [15], RDX [16], hexanitrohexaazatetracyclododecane (CL-20) [17], hydroxy-terminated polybutadiene (HTPB) [18–20], Ammonium Perchlorate (AP) [18, 21], Ammonium Nitrate (AN) [22], triaminotrinitrobenzene (TATB) [23] are some of the monomolecular energetic compounds [24]. But their limited energy density and difficulty in tweaking their performances for safety, sensibility, and stability reasons [25] led to development of a new class of energetic composite materials, i.e., nanothermites.

2.2. Composite energetic materials

Composite Energetic materials, also known as Heterogeneous Reactive Materials [14] are physical mixtures of metal-fuel powders, namely, Aluminum [26], Titanium [27], Zirconium [28], Boron, Magnesium [29], Silicon [30–32], Chromium and oxidizer powders, namely, CuO [18, 33].

Fe_2O_3 [34–36], Bi_2O_3 [37, 38], WO_3 [39] etc. which undergo exothermic redox reaction thus liberating a significant amount of energy with temperatures around 3000 K or more [40]. As compared to monomolecular EMs, composite EMs have high combustion enthalpies (figure 1) [41] and energy densities (figure 2) [42]. Their ability to be tailored as per the properties required for the application makes them a promising candidate for a variety of applications.

2.2.1. Al-based energetic materials

Of all the metals, Aluminum ordinarily serves to be a suitable candidate as metal fuel. Earth's crust is rich with aluminum, thus making it the third most copiously found element. It has high reactivity and characterized by high heat and efficient combustion, a high specific energy density of approximately 30 kJ g^{-1} , high enthalpy,

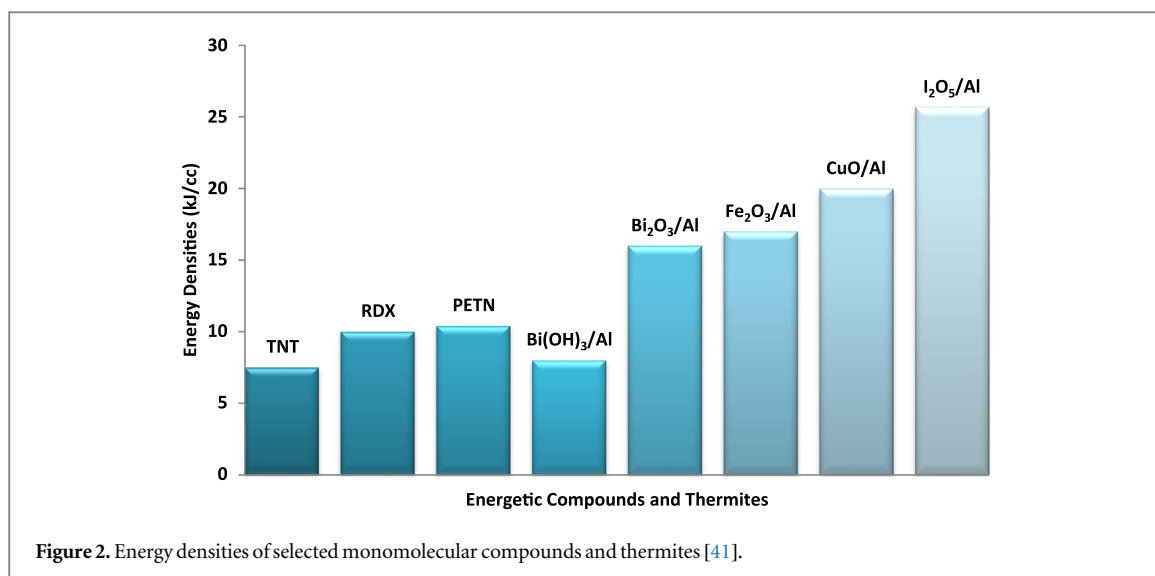


Figure 2. Energy densities of selected monomolecular compounds and thermites [41].

high calorific value, and so forth [16, 43, 44]. Al augments the material's reactive power by escalating the combustion velocity by virtue of its high thermal conductivity [45]. Since it is non-toxic and shows excellent catalytic behavior, Aluminum is perpetually employed as a competent metallic fuel in composite EMs [1, 46, 47].

The aluminum powder acts as a crucial element in pyrotechnics, rocket propellants, and explosives. The factors like particle size and aluminum content should be considered judiciously as it affects the burning time, ignition delay time, viscosity of a rocket propellant mixture, specific impulse (I_{sp}), and ignition temperature.

2.2.1.1. Micron-sized particles

Several researchers have fabricated energetic composite materials by incorporating micron-sized particles [48, 49]. Gibot *et al* [50] assessed the pyrotechnic performance for Al/SnO₂ energetic composite system comprised of SnO₂ with particle size <10 μm and Al particles with size ~50 nm with the equivalence ratio (ϕ) ranging between from 0.8 to 1.8. The combustion velocities ranged from 480 m s^{-1} to optimum value of approximately 580 m s^{-1} for equivalence ratio between 1 to 1.4. Equivalence ratio [48, 50, 51] is computed as:

$$\phi = \frac{(F/A)_{act}}{(F/A)_{st}} \quad (1)$$

where F = fuel, A = oxidizer, act and st in the subscript indicate the real and stoichiometric ratios, respectively.

In another study, Kang *et al* [28] successfully synthesized micron-sized Potassium Perchlorate and Zirconium (KClO₄/Zr) composite by employing a chemical solution - deposition method. As the amount of KClO₄ varied (38 wt%, 42 wt %, 71 wt %), different structures were observed, as shown in figure 3. (~6 μm) KClO₄/Zr (3–6 μm) composites displayed an extended light-radiation period and greater light-radiation energy/power. Whereas, Brown *et al* has enlisted experimental burning rates for a variety of binary pyrotechnic combinations with different compositions having different fuel particles size (in microns). For instance, reduction in the fuel particles radius from 14 μm to 2 μm while keeping the constant oxidizer particle radius in the Sb/KMnO₄ (13 μm) system [30], led to a rise in the burning rate ranging from 2 mm s^{-1} to 8 mm s^{-1} . Similarly, the decrease in the fuel particle radius of Mo from ~18 μm to 7 μm in the Mo/peroxide systems like Mo/SrO₂ (~2 μm), Mo/BaO₂ (~5 μm) showed a substantial boost in the experimental burning rate values. Thus, it is ascertained that diminution in the particle size leads to a significant improvement in the desirable properties of the composite systems. Unlike the inadequacies like high ignition temperature, particle agglomeration, low energy release rate of micron-sized particles, researchers moved on towards using nanoparticles (figure 4) [52, 53].

2.2.1.2. Nano-sized particles/Nanothermites

Nanothermite is a metastable intermolecular composite (MIC) [54–56] comprising of metal oxides and metallic fuel with their particle size ranging in the nanometric scale (1–100 nm).

Standard equation of a thermite reaction [57] is as follows:



Some of the thermite reactions along with their adiabatic reaction temperature, heat of reaction and generation of gas have been given in table 1 [12]. The parameters, namely, ignition temperature, reaction rate, combustion

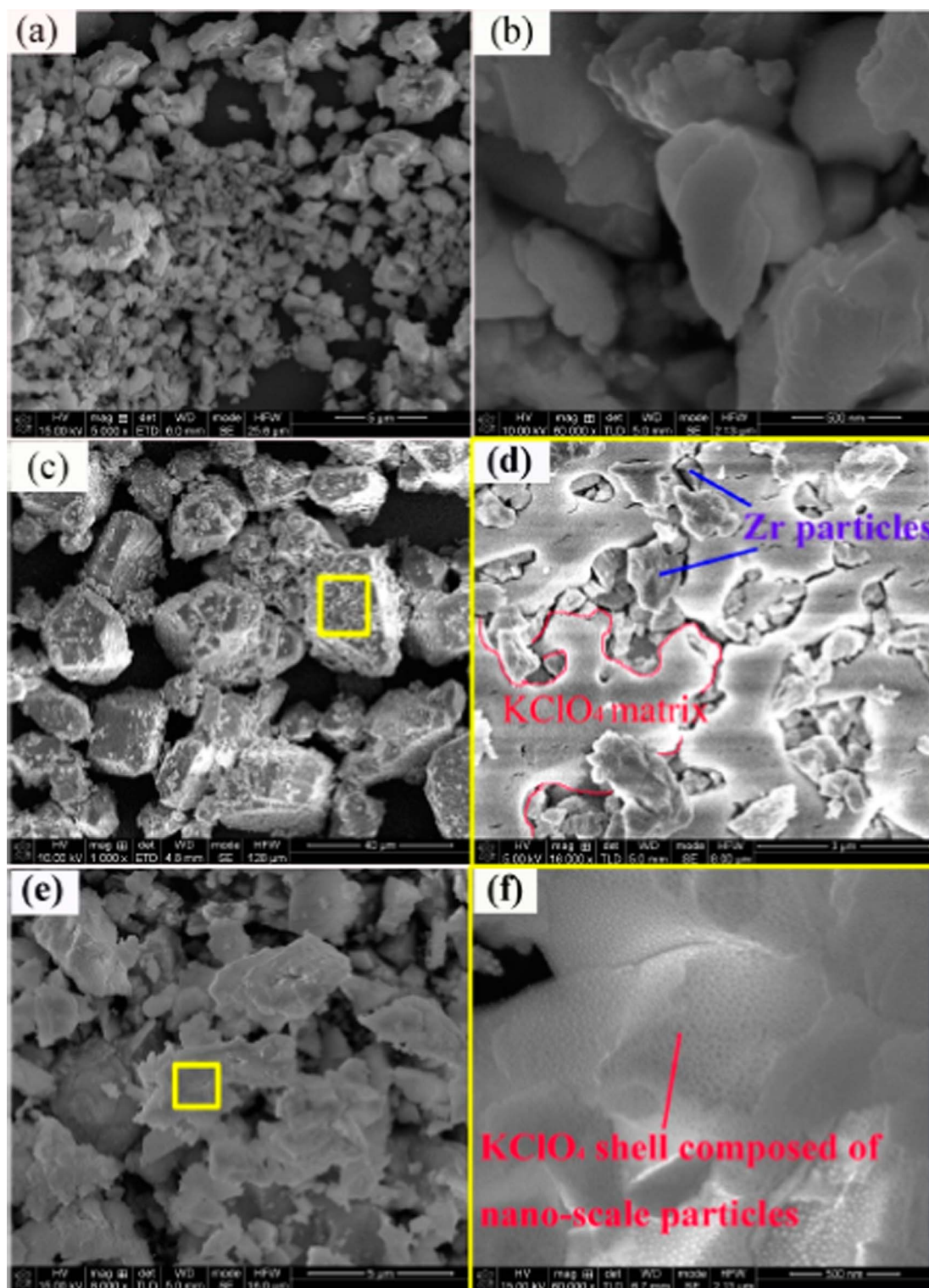


Figure 3. (a) Surface of Zr powder of 3 μm , (b) Zr particles showing even surface, (c) KClO_4/Zr (3 μm) (71/29, wt.%) composite, (d) embedded structure of Zr particles in KClO_4 matrix (e) KClO_4/Zr (3 μm) (38/62, wt.%) composite (f) thin shell of KClO_4 with nanometer particles [28]. (Open access CC BY 4.0).

velocities, ignition time and decomposition temperature in pyrotechnic mixtures get influenced by the reduced size of the fuel and oxidizer particles and show significant improved properties. Nanothermites/MICs are also called as Superthermites depending upon the extent of reactivity. Nanoparticles, unlike microparticles, increase the intimate interaction between oxidizer and fuel, that lessens the diffusion distance for mass transport, thus accelerating the reaction or burning rate [42] and reducing the mechanical sensitivity and ignition time [12]. They have increased ignition sensitivity due to its high specific surface area [58], the surplus energy of surface atoms, and strong surface activity. Pantoya *et al* performed a study on the effect of nano and micron fuel particles

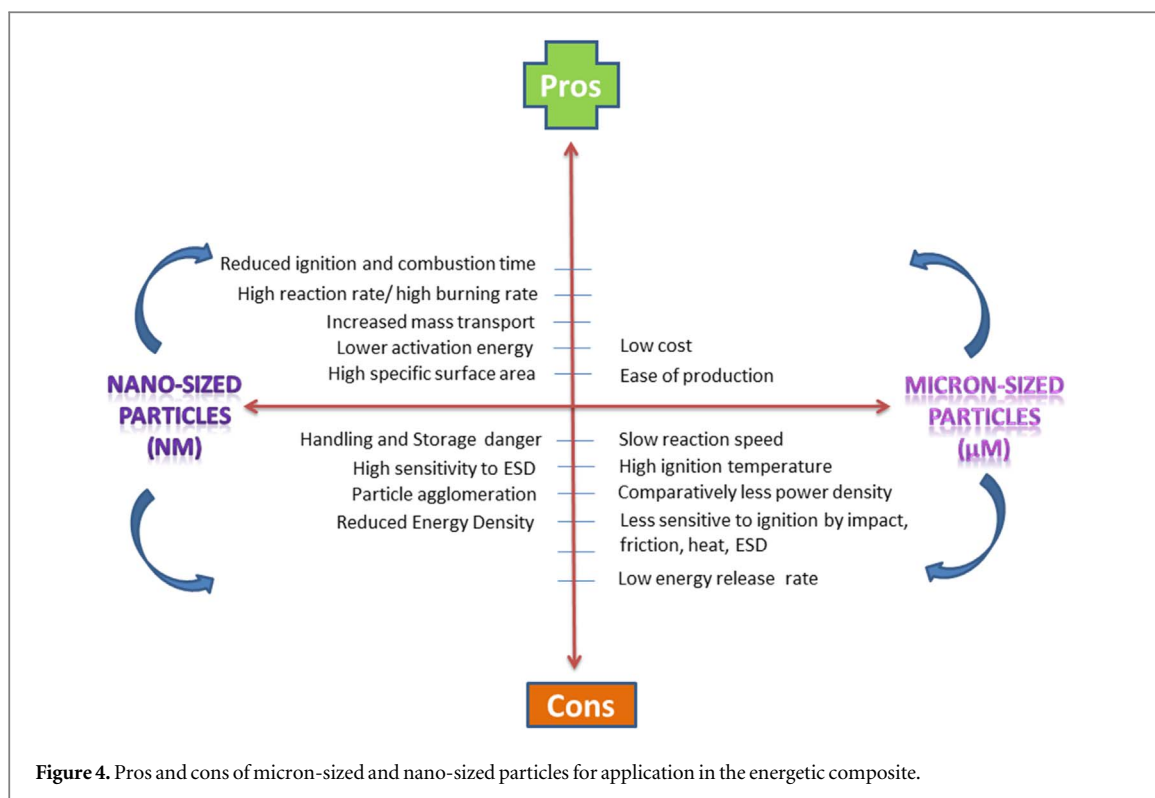


Table 1. Thermophysical properties of Thermite reaction [12]. Reprinted with permission. Copyright Elsevier 2017.

| Reactants Constituents | Adiabatic reaction temperature (K) | | Production of gas | | Heat of reaction | |
|---------------------------------------|------------------------------------|-----------------------|-------------------|--------------------|---------------------|--------------------|
| | Density | Without phase changes | g of gas/g | Moles of Gas/100 g | kJ cm ⁻³ | kJ g ⁻¹ |
| 2Al + Cr ₂ O ₃ | 4.190 | 2789 | 0 | 0 | 10.9 | 2.6 |
| 2Al + 3CuO | 5.109 | 5718 | 0.3431 | 0.5400 | 20.8 | 4.1 |
| 2Al + 3Cu ₂ O | 5.280 | 4132 | 0.0776 | 0.1221 | 12.7 | 2.4 |
| 2Al + Fe ₂ O ₃ | 4.175 | 4382 | 0.0784 | 0.1404 | 16.5 | 4.0 |
| 8Al + 3Fe ₃ O ₄ | 4.264 | 4075 | 0.0307 | 0.0549 | 15.7 | 3.7 |
| 4Al + 3MnO ₂ | 4.014 | 4829 | 0.4470 | 0.8136 | 19.5 | 4.8 |
| 2Al + MoO ₃ | 3.808 | 5574 | 0.2473 | 0.2425 | 17.9 | 4.7 |

on the combustion velocities as shown in figure 5 which shows the dependence of combustion velocity on the Al particle size [48].

However, the synthesis of the nanoparticles can be done using various processing techniques. Aluminum nanoparticles were synthesized by the vapor phase condensation method by Schefflan *et al* [59]. The vapor deposition method produces nano-sized metal particles by cooling the gaseous form of the metal that is carried away by an inert gas. Whereas, Electrical Explosion of Wires (EEW) [41, 60, 61] technique was one of the other methods used to obtain ultra fine metal powders. This method is characterized by high voltage source to generate high current pulses of about thousands of amperes, high plasma temperatures (~10000 K), pulse duration ranging from μ s to nanoseconds. Accordingly, it proves to be more advantageous than other evaporation methods as the electrical energy gets directly transmitted into heat. Furthermore, Elbasuney *et al* employed the hydrothermal synthesis method for fabricating colloidal CuO and Fe₂O₃ nanoparticles for their integration in the energetic systems [12], as shown in figure 6. CuO and Fe₂O₃ are the most commonly used metal oxides for energetic applications.

Similarly, the hydrothermal method [62] was also used to prepare nano-bismuth oxide particles having size of around 47 nm by Wang *et al*. This method involved preparing a mixture by adding 2.425 g of Bi(NO₃)₃·5H₂O to 10 ml of (CH₂OH)₂, which is further stirred with C₂H₅OH for 30 min. This solution is then transferred to autoclaves and heated for 10 h at ~160 °C. Upon cooling, they were washed with deionized water and alcohol, respectively. Drying for 6 h at 60 °C and calcination for 2 h at 325 °C eventually produces nano Bi₂O₃ particles.

On the other hand, Chowdhury *et al* synthesized nano Fe₂O₃ particles by polymer matrix encapsulation technique for their use as an oxidizer for energetic applications [63]. Depending on the Fe³⁺ concentration, the

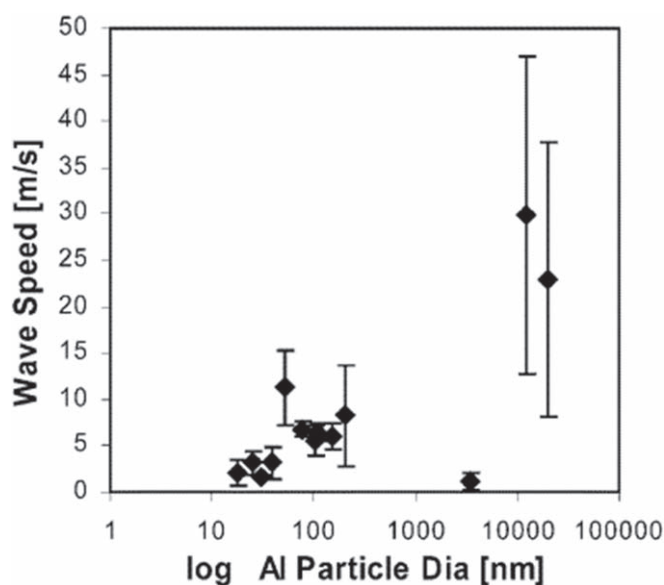


Figure 5. Combustion velocity as a function of Al particle on log scale [48]. Reprinted with permission. Copyright John Wiley and Sons 2005.

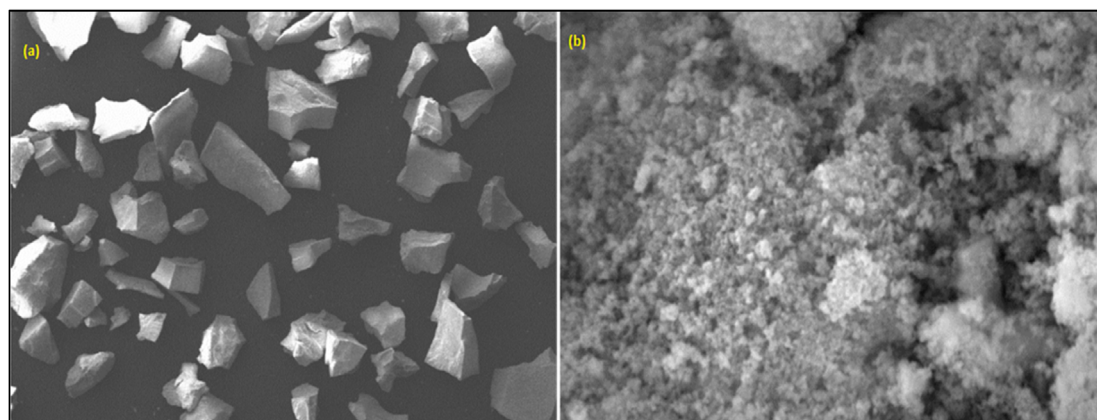


Figure 6. SEM micrographs of (a) Fe_2O_3 and (b) CuO nanoparticles [12]. Reprinted with permission. Copyright Elsevier B.V. 2017.

Fe_2O_3 particle of 30 nm size shows the specific surface energy of $24 \text{ m}^2 \text{ g}^{-1}$ to $126 \text{ m}^2 \text{ g}^{-1}$. Cheng *et al* fabricated novel Fe_2O_3 nanotubes–Al nanoparticles superthermites by employing the surfactant self-assembly process, which is a remarkable method as the relative arrangement of the fuel with oxidizer shows upgraded reaction and burning characteristics [64]. Kim *et al* analyzed the combustion and ignition properties of Al microparticles (MPs)/Al nanoparticles (NPs)/ Fe_2O_3 nanoparticles (NPs), as depicted in figure 7 [34].

Some of the different composite systems reinforced with nanoparticles of metal fuel or oxidizers, their comparison and influence on the properties and have been discussed. Sanders *et al* analyzed the optimization of composites like Al/ MoO_3 , Al/ CuO , Al/ WO_3 , and Al/ Bi_2O_3 as regards to the propagation speed (or burn rate) pressure output. It was concluded that the propagation depends on the state of the products and produced gas. Higher gas generation and liquid or gas products leads to higher propagation speed [65]. Besides, Glavier *et al* [66] performed a comparative analysis of burning rates, pressure peaks, and pressurization rate of the nanocomposites. The burning rate varied from 65 m s^{-1} (Al/ CuO foils) to 420 m s^{-1} (Al/ Bi_2O_3). The pressurization rate was maximum for Al/ Bi_2O_3 nanocomposite with a value of approximately $5760 \text{ kPa} \cdot \mu\text{s}^{-1}$ at 30% TMD. Whereas the pressure peak of 41.7 MPa were reported to be highest at 50% TMD for Al/ CuO . Figure 8. displays the SEM images for all the four energetic composite system.

Bockmon *et al* showed the impact of particle size on the pressure and combustion velocities of Al/ MoO_3 metastable interstitial composites. Upon reducing the particle size from 121 nm to 44 nm, the combustion velocities showed a rise in the combustion velocity values from 600 m s^{-1} to 1000 m s^{-1} , respectively, as shown

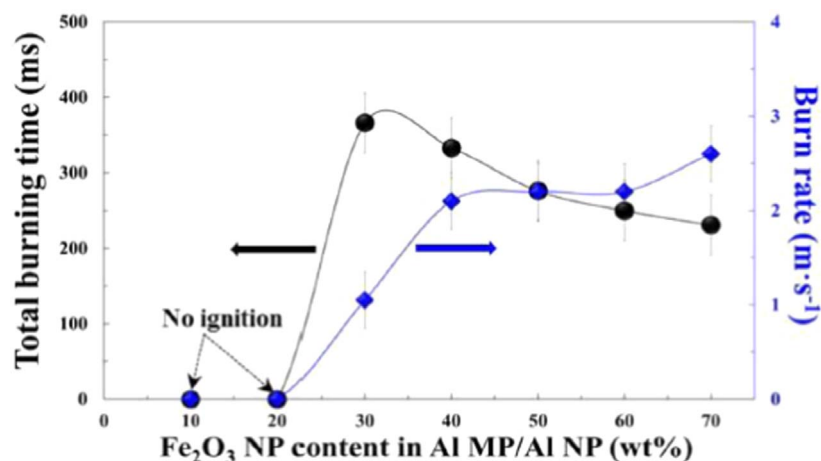


Figure 7. Burning rate and time per the variation in the Fe₂O₃ content in Al (MP)/Fe₂O₃ and Al(NP)/Fe₂O₃ composites [34]. Reprinted with permission. Copyright Elsevier 2018.

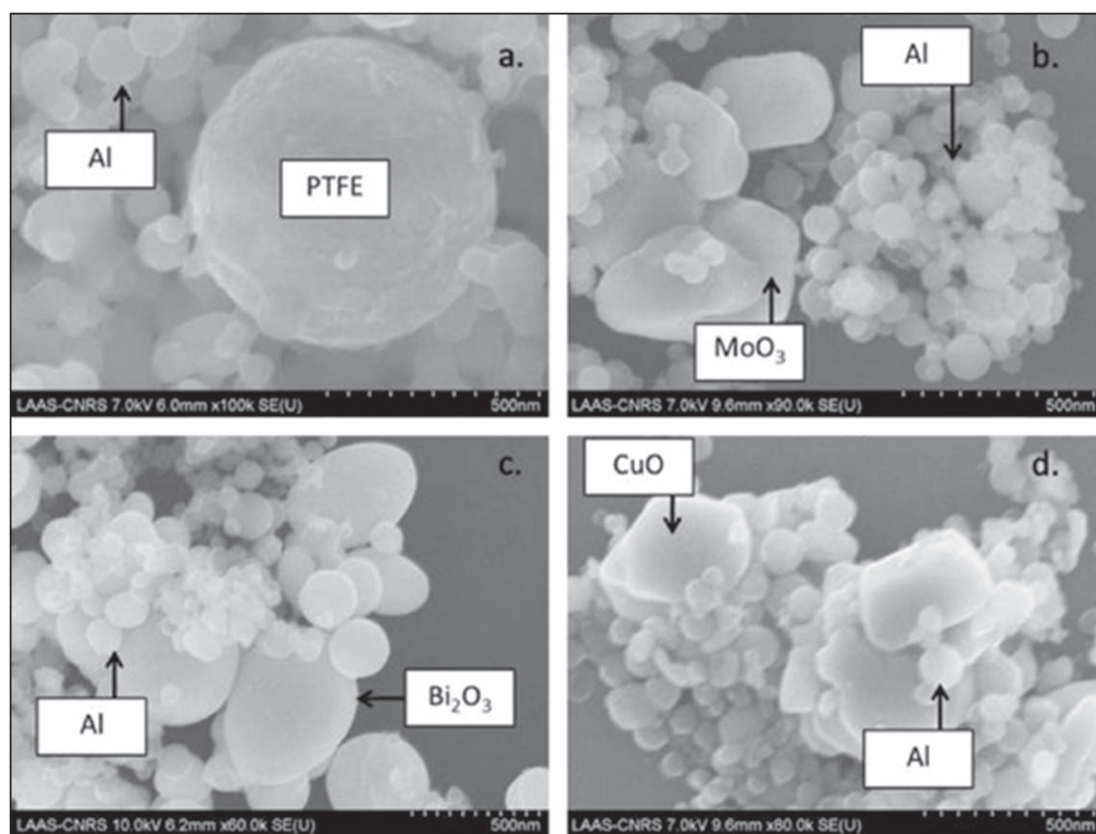


Figure 8. SEM images of (a) Al/PTFE, (b) Al/MoO₃, (c) Al/Bi₂O₃, (d) Al/CuO NPs [66]. Reprinted with permission. Copyright Elsevier Inc. 2015.

in table 2 [40]. Additionally, Granier and Pantoya [67] performed a comparative analysis of the ignition times for the nanoAl/MoO₃ and micro Al/Mo₄ energetic systems. The results reveal that the ignition times reduce significantly from 6 s for micron-sized ($\sim 20 \mu\text{m}$) Al particle composites up to 12 ms for nanothermites ($\sim 17 \text{ nm}$). As depicted in table 3 [67], the burn rates showed an increase from 4 m s^{-1} to 12 m s^{-1} when the size of aluminum particles was reduced from 200 nm to 50 nm.

2.2.2. Si-based energetic systems

Aluminum nanoparticles having average size of 80 nm show high electrostatic discharge sensitivity and at a very low discharge energy level of 0.98 mJ, it tends to ignite. Thus, Thiruvengadathan *et al* [51] developed Silicon-

Table 2. Combustion velocity and pressure values for Sample A (particle diameter = 44 nm), Sample B (particle diameter = 80 nm), Sample C (particle diameter = 121 nm) [40]. Reprinted with permission. Copyright AIP Publishing 2005.

| Density | | Sample A | Sample B | Sample C |
|---------|---|----------|----------|----------|
| Low | Average (Avg.) velocity (m s^{-1}) | 959.3 | 988.7 | 684.4 |
| | Standard deviation (Std. dev.) | 35.4 | 135.6 | 81.8 |
| | Pressure (MPa) | 10.8 | 12.4 | 10.9 |
| | Std. dev. | 0.8 | 3.6 | 1.3 |
| | Mass rate (g s^{-1}) | 2308 | 2665 | 1794 |
| Medium | Avg. velocity | 916.0 | 988.3 | 784.7 |
| | Std. dev. | 59.4 | 56.9 | 57.0 |
| | Pressure (MPa) | 17.5 | 16.5 | 12.4 |
| | Std. dev. | 1.4 | 2.5 | 1.8 |
| | Mass rate (g s^{-1}) | 2805 | 3230 | 2522 |
| High | Avg. velocity | 950.7 | 948.7 | 765.3 |
| | Std. dev. | 46.1 | 37.0 | 22.5 |
| | Pressure (MPa) | 22.1 | 17.9 | 18.6 |
| | Std. dev. | 4.5 | 1.2 | 1.8 |
| | Mass rate (g s^{-1}) | 3600 | 3607 | 2856 |

Table 3. Ignition time and Combustion wave speed of Al/MoO₃ influenced by the particle size [67]. Reprinted with permission. Copyright Elsevier 2004.

| Al particle diameter (nm) | Burn rate | | Ignition time | |
|---------------------------|-------------------------------|--------------------------------------|---------------|---------------------|
| | Average (m s^{-1}) | Std. deviation (m s^{-1}) | Average (ms) | Std. deviation (ms) |
| 17.4 | 2.16 | 1.39 | 24.21 | 8.76 |
| 24.9 | 3.23 | 1.27 | 21.73 | 12.60 |
| 29.9 | 1.64 | 0.14 | 18.39 | 10.38 |
| 39.2 | 3.17 | 1.75 | 21.93 | 12.00 |
| 52.7 | 11.23 | 4.12 | 15.55 | 6.57 |
| 75.9 | 6.81 | 0.73 | 20.76 | 6.90 |
| 100.9 | 5.55 | 1.65 | 14.56 | 4.69 |
| 108 | 6.40 | 0.96 | 17.31 | 4.37 |
| 153.8 | 6.04 | 1.33 | 25.49 | 11.88 |
| 202 | 8.26 | 5.48 | 12.40 | 2.68 |
| 3000–4000 | 1.20 | 0.85 | 89.43 | 52.82 |
| 10,000–14,000 | 29.92 | 17.14 | 1384.13 | 736.05 |
| 20,000 | 22.91 | 14.89 | 6039.43 | 847.18 |

based nanoenergetic composite that displays decreased sensitivity and because of its property of surface passivation are capable of replacing aluminum nanoparticles in specific applications requiring lower combustion performance. The highest pressurization rate of $\sim 2.7 \text{ MPa } \mu\text{s}$ and combustion wave speed from 1200 to 1500 m s^{-1} were reported as a function of equivalence ratio ($\phi = 0.9$).

Brown *et al* [30] did a comprehensive study on Si-based and other fuel/oxidant systems. It was assumed that particles of fuel and oxidant are spherical in order to calculate the total number of point of contact (N_R) between them and compare it with the experimental burn rates of Si/Pb₃O₄, Sb/KMnO₄, Si/Fe₂O₃, Si/Sb₂O₃, Si/KNO₃ pyrotechnic mixtures. The results of those fuel/oxidant systems have been represented in tables 4–6 [30]. It was concluded from the results that a minute variation in size of particle dramatically influences the contact points of fuel-oxidizer, and accordingly shows a significant influence on combustion velocity.

2.2.3. Hybrid/other composite systems

Recently, Wang *et al* [68] succeeded in incorporating ammonium perchlorate (AP) to a composite of fluoropolymer named polytetrafluoroethylene (PTFE) and Aluminum. This 9 wt% addition of AP to PTFE/Al energetic composite displayed substantial escalation in the output of energy (8863 J g^{-1}), burn rate (1626 m s^{-1}) and pressurization rate (340 MPa ms^{-1}) as compared to pure PTFE/Al which has output of energy of 2019 J g^{-1} , burn rate of 260 m s^{-1} and pressurization rate 29.3 MPa ms^{-1} (figures 9–11).

A far greater burn rate and totally different flame structure are seen for PTFE/Al with AP, which shows that introduction of AP possibly enhances energy output [68] and combustion kinetics. Zamkov *et al* [69]

Table 4. Calculated point of contact (N_R) and experimental burning rates (ν) for Si/Pb₃O₄ system [30]. Reprinted with permission. Copyright John Wiley and Sons 1999.

| Pb ₃ O ₄ r = 2.5 μ m | | | | | | |
|---|--------------------------------|----------------------------|----------------------------|----------------------------|----------------------------|----------------------------|
| r r _{fuel} :r _{oxidant} %Si | Si sample (A) | | Si sample (B) | | Si sample (C) | |
| | 1.0 μ m | | 2.0 μ m | | 2.5 μ m | |
| | 1:2.5 | | 1:1.3 | | 1:1 | |
| | ν (mm s ⁻¹) | N_R ($\times 10^9$) | N (mm s ⁻¹) | N_R ($\times 10^9$) | N (mm s ⁻¹) | N_R ($\times 10^9$) |
| 5 | 108.9 | 18.3 | 46.1 | 4.3 | 42.4 | 2.8 |
| 10 | 222.2 | 26.6 | 94.4 | 7.0 | 64.6 | 4.8 |
| 15 | 257.4 | 30.2 | 100.6 | 8.7 | 71.5 | 6.1 |
| 20 | 249.9 | 31.7 | 108.7 | 9.8 | 79.9 | 6.9 |
| 25 | 138.8 | 31.8 | 134.3 | 10.3 | 98.7 | 7.4 |
| 30 | 139.0 | 31.1 | 163.0 | 10.5 | 114.8 | 7.7 |
| 35 | 127.1 | 29.9 | 116.6 | 10.4 | 86.6 | 7.7 |
| 40 | 114.7 | 28.4 | 89.4 | 10.2 | 72.3 | 7.6 |
| 45 | 94.4 | 26.6 | 69.2 | 9.7 | 53.2 | 7.3 |
| 50 | 59.3 | 24.6 | 38.8 | 9.2 | — | 7.0 |
| 55 | — | 22.5 | — | 8.5 | — | 6.5 |
| 60 | — | 20.2 | — | 7.8 | — | 6.0 |
| 65 | — | 17.9 | — | 7.0 | — | 5.4 |
| 70 | — | 15.5 | — | 6.1 | — | 4.7 |
| 75 | — | 13.0 | — | 5.2 | — | 4.0 |
| 80 | — | 10.5 | — | 4.2 | — | 3.3 |
| 85 | — | 7.9 | — | 3.2 | — | 2.5 |
| 90 | — | 5.3 | — | 2.2 | — | 1.7 |
| 95 | — | 2.7 | — | 1.1 | — | 0.9 |

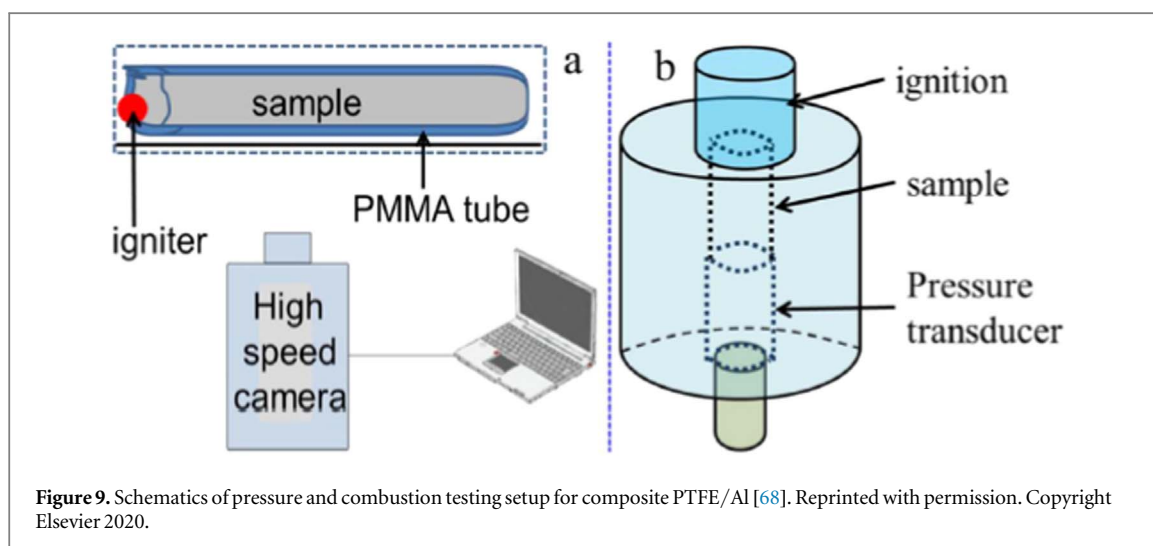
Table 5. Calculated point of contact (N_R) and experimental burning rates (ν) for Si/SnO₂, Si/Fe₂O₃, Si/Sb₂O₃, Si/KNO₃ system [30]. Reprinted with permission. Copyright John Wiley and Sons 1999.

| Si sample(3) r _{fuel} = 1.7 μ m | | | | | | | | |
|---|--------------------------------|-------------------------------|-----------------------------------|-------------------------------|-----------------------------------|-------------------------------|----------------------------|-------------------------------|
| r _{fuel} /r _{oxidant} %Si | Si/SnO ₂ | | Si/Fe ₂ O ₃ | | Si/Sb ₂ O ₃ | | Si/KNO ₃ | |
| | 3.8 | | 5.7 | | 1.4 | | 0.25 | |
| | ν (mm s ⁻¹) | N_R ($\times 10^{10}$) | N (mm s ⁻¹) | N_R ($\times 10^{10}$) | ν (mm s ⁻¹) | N_R ($\times 10^{10}$) | N (mm s ⁻¹) | N_R ($\times 10^{10}$) |
| 10 | — | 11.6 | — | 23.5 | — | 2.68 | — | 0.704 |
| 15 | — | 16.9 | — | 34.7 | — | 3.69 | — | 0.907 |
| 20 | 5.25 | 21.7 | 2.33 | 45.5 | 1.56 | 4.50 | — | 1.03 |
| 25 | 7.54 | 26.0 | 3.67 | 55.8 | 3.25 | 5.13 | — | 1.10 |
| 30 | 11.6 | 29.8 | 3.82 | 65.6 | 6.30 | 5.58 | 1.65 | 1.13 |
| 35 | 14.8 | 33.0 | 3.60 | 74.7 | 8.71 | 5.89 | — | — |
| 40 | 17.1 | 35.6 | 4.54 | 83.1 | 8.52 | 6.05 | 2.78 | 1.10 |
| 45 | 15.7 | 37.6 | — | 90.5 | 8.73 | 6.08 | — | — |
| 50 | 12.8 | 38.8 | — | 96.9 | 7.25 | 5.98 | 4.96 | 0.995 |
| 55 | 9.11 | 39.2 | — | 102 | — | 5.78 | — | — |
| 60 | — | 38.7 | — | 105 | — | 5.46 | 8.43 | 0.844 |
| 65 | — | 37.3 | — | 107 | — | 5.06 | — | — |
| 70 | — | 35.0 | — | 106 | — | 4.56 | 10.7 | 0.661 |
| 75 | — | 31.5 | — | 102 | — | 3.98 | 17.1 | 0.560 |
| 80 | — | 27.0 | — | 93.7 | — | 3.32 | 20.6 | 0.455 |
| 85 | — | 21.4 | — | 80.1 | — | 2.58 | 34.5 | 0.346 |
| 90 | — | 14.8 | — | 59.8 | — | 1.78 | — | 0.234 |

investigated the chemistry involved in Al/Teflon^{AF} nanoenergetic material using Ultrafast mid-infrared (IR) spectroscopy, where Teflon^{AF} is a copolymer of tetrafluoroethylene (TFE) and 2,2-bis(trifluoromethyl)-4,5-difluoro-1,3-dioxole (dioxole). As compared to the theoretical value of heat of combustion of 8 kJ cm⁻³ for TNT, Al/Teflon mix shows a significantly high value of 21 kJ cm⁻³.

Table 6. Calculated point of contact (N_R) and experimental burning rates (ν) for Sb/KMnO₄ syste [30]. Reprinted with permission. Copyright John Wiley and Sons 1999.

| | | | | | | |
|--|--------------------------------|----------------------------|--------------------------------|----------------------------|--------------------------------|----------------------------|
| KMnO ₄ $r = 13 \mu\text{m}$ | | | | | | |
| r | Sb sample (1) | | Sb sample (3) | | Sb sample (4) | |
| | 13 μm | | 9 μm | | 3 μm | |
| | 1.0 | | 0.69 | | 0.23 | |
| $r_{\text{fuel}}/r_{\text{oxidant}}$ | | | | | | |
| %Sb | | | | | | |
| | ν (mm s ⁻¹) | N_R ($\times 10^7$) | ν (mm s ⁻¹) | N_R ($\times 10^7$) | ν (mm s ⁻¹) | N_R ($\times 10^7$) |
| 10 | — | 1.6 | — | 3.4 | — | 50 |
| 20 | — | 3.1 | — | 6.4 | — | 86 |
| 30 | 2.0 | 4.3 | 2.5 | 8.8 | 6.5 | 105 |
| 35 | 2.5 | — | 4.3 | — | 8.4 | — |
| 40 | 5.5 | 5.3 | 7.0 | 10.6 | 12.5 | 111 |
| 50 | 10.0 | 6.0 | 11.5 | 11.6 | 19.0 | 106 |
| 60 | 11.0 | 6.3 | 11.0 | 11.8 | 20.5 | 94 |
| 70 | 9.5 | 6.1 | 11.0 | 10.9 | 22.5 | 77 |
| 80 | — | 5.2 | — | 8.8 | — | 54 |
| 90 | — | 3.3 | — | 5.3 | — | 29 |



Zhu *et al* did the latest study on hybrid nanothermite composites fabricated on a substrate (silicon) by lodging CL-20 with arrays of CuO/Al nanothermite. The properties of heat release were upgraded with 18.2% decrease in activation energy of integrated CL20 and increase in the total heat of reaction. The synthesized nanoenergetic composite shows an appropriate behavior of burning with an intense yet stable combustion flame [70].

3. Synthesis and properties of energetic materials

3.1. Evaporation-assisted (Vapor deposition)

Layered vapor deposition usually is an adaptable process as nearly all the recurrently used metalloids, metal oxides and metals are able to be made by selecting appropriate deposition factors with easy control over the layer thicknesses. In the interim, the dense and distinct reactive multilayer nano foil (RMF) geometry makes the theoretical modeling more simple and boosts accuracy but this technology has some constraints. This method is expensive and challenging to scale up. Moreover, the problem of premixing becomes severe with minimal bilayer spacing. The interfacial free energies, chemical, and elastic strain can obliterate the structure of the layers. Conclusively, when total RMF is exceptionally thick, the unpredictability is a matter of concern, when reactants with diverse properties or with substrates are deposited. Manesh *et al* employed a magnetron sputter deposition method to prepare a layered Al/CuO films of thickness upto 3 μm [71]. Likewise, Petrantonio *et al* [72] deposited micro/nanostructured thermite of Al/CuO on SiO₂ wafers as displayed in figure 12 [72].

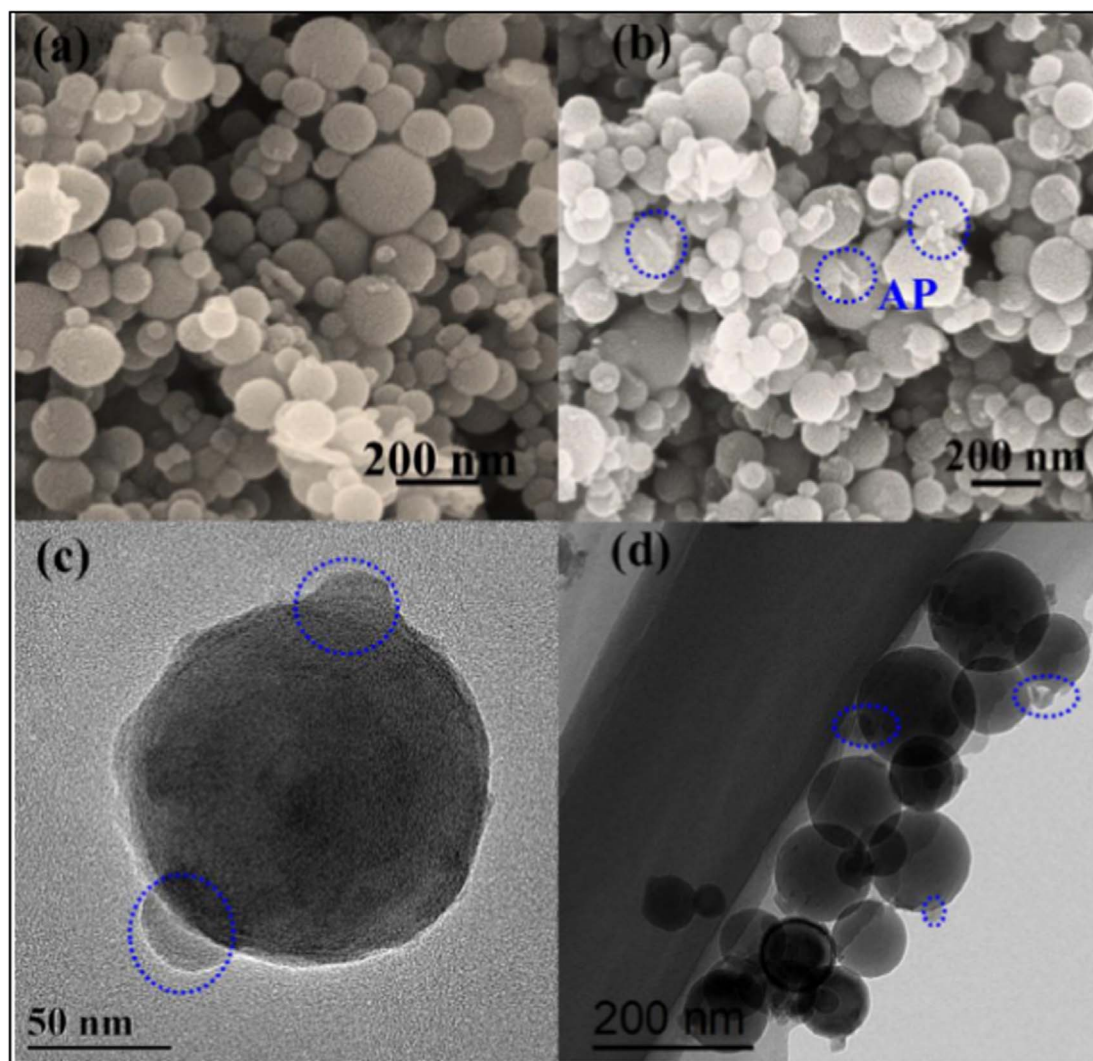


Figure 10. FE-SEM images of (a) PTFE/Al with AP, (b) TEM image of PTFE and nano AP, (c) PTFE/Al with nano AP, (d) AP in PTFE/Al display irregularity of size ~ 50 nm [68]. Reprinted with permission. Copyright Elsevier 2020.

Ferguson *et al* made use of the atomic layer deposition (ALD) process to sequentially deposit thin and uniform layers of SnO_2 onto Al nanoparticles (diameter ~ 50 nm) to prepare the Al/ SnO_2 nanothermite with the help of H_2O_2 and SnCl_4 reactants in a fluidized bed reactor [73]. ALD is considered to be an ideal process due to its self-terminating surface chemical reaction mechanism that involves purging in of inert gases after every pulse of the precursors which lead to high conformality and uniformity in the thickness of the thin deposited films. Upon ignition, it was observed that the SnO_2 coated Al particles reacted intensely as compared to uncoated Al particles thus demonstrating that ALD method can be utilized in fabrication of improved thermite systems.

3.2. Sol-gel technique

The sol-gel process includes chemical reactions taking place in the solution for initial production of nanoparticles called as 'sols' that are connected in a 3D solid system, called as 'gel', and the remaining solution is filled in the open pores. Figure 13 represents the sol-gel methodology [74, 75]. Primarily there are three steps in sol-gel procedure; hydrolysis, condensation and drying. The sol-gel process is comparatively an easy method executed at low temperatures, relatively economical and it has the potential of producing utterly novel energetic materials with sought after properties [74].

Comparative study of sol-gel Ta/ WO_3 nanocomposites with conventional powder mixtures was done. This study revealed that the heat released by sol-gel composite was approximately 30% to 35% greater as compared to the powder mixture due to the carbon presence in the sol-gel composite. In addition, Ta/ WO_3 nanocomposite produced by the sol-gel were found to be unresponsive to spark, friction and impact ignition [76, 77].

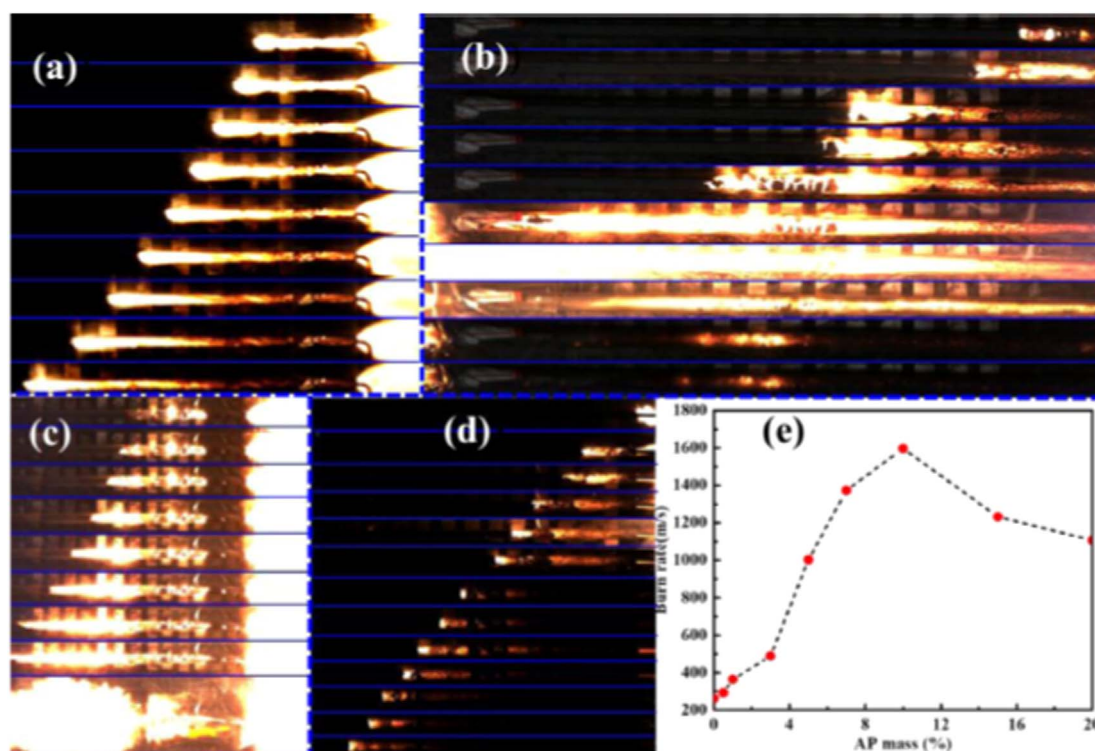


Figure 11. Flame propagation pictures of (a) PTFE/Al, (b) PTFE/Al with (6 wt%)AP, (c) PTFE/Al with (9 wt%)AP, (d) PTFE/Al with (14 wt%)AP, (e) quantity of AP affects burn rate of PTFE/Al [68]. Reprinted with permission. Copyright Elsevier 2020.

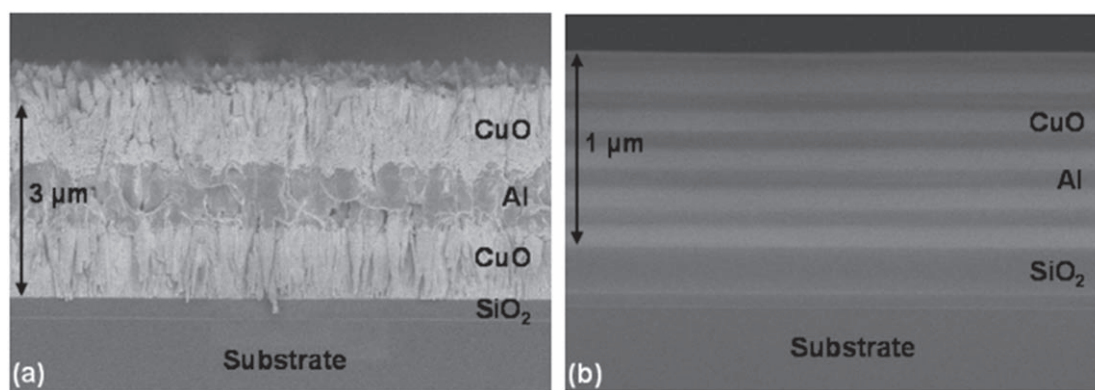


Figure 12. Cross-sectional SEM images of multilayers magnetron sputtered (a) 3 layers of 1 μm each of CuO/Al/CuO, (b) 10 layers of 100 nm each of CuO/Al [72]. Reprinted with permission. Copyright AIP Publishing 2010.

3.3. High-energy ball milling: arrested reactive milling (ARM)

Ward *et al* produced micron-sized energetic composite powders using arrested reactive milling of Aluminum and metal oxides like MoO₃ and Fe₂O₃ [78]. Arrested reactive milling [41, 58, 79] works on the principle of discontinuing the exothermic reactions just before the mechanical initiation due to high-energy milling [80] of powders (figures 14 and 15) [58].

3.4. Electrophoretic deposition

Electrophoretic deposition [31, 81, 82] is an effective method used to make films on different surfaces of the conductive materials. Figure 16 shows the electrophoretic deposition setup arrangement [83]. The composition and quality of deposited coatings can be quantitatively altered by regulation of concentration of charged particles, time of deposition and field strength. It has extensive use for deposition of charged particles over irregular substrate surfaces and as anticorrosive coatings. Lately, Wang *et al* explored the exothermic and

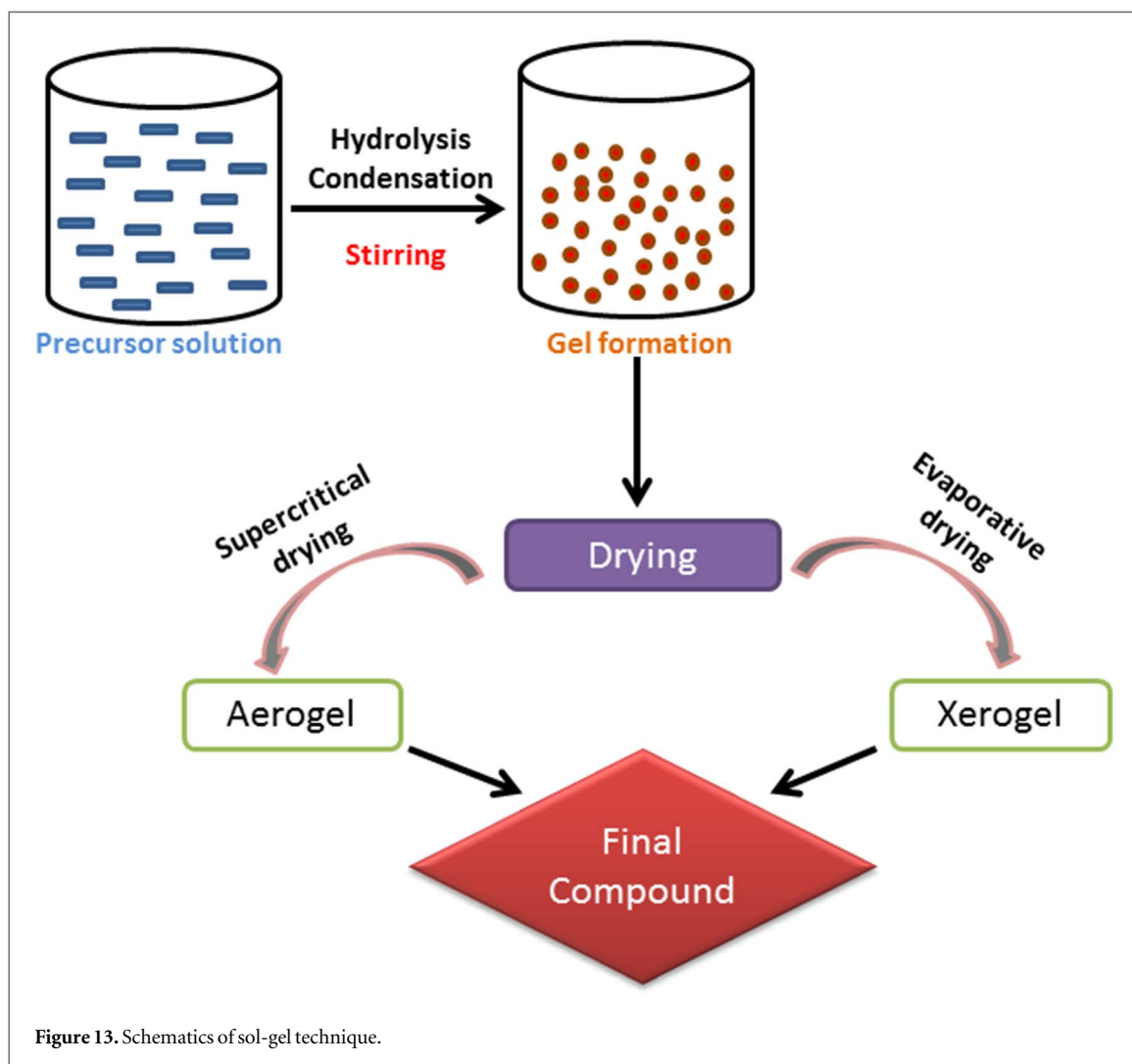


Figure 13. Schematics of sol-gel technique.

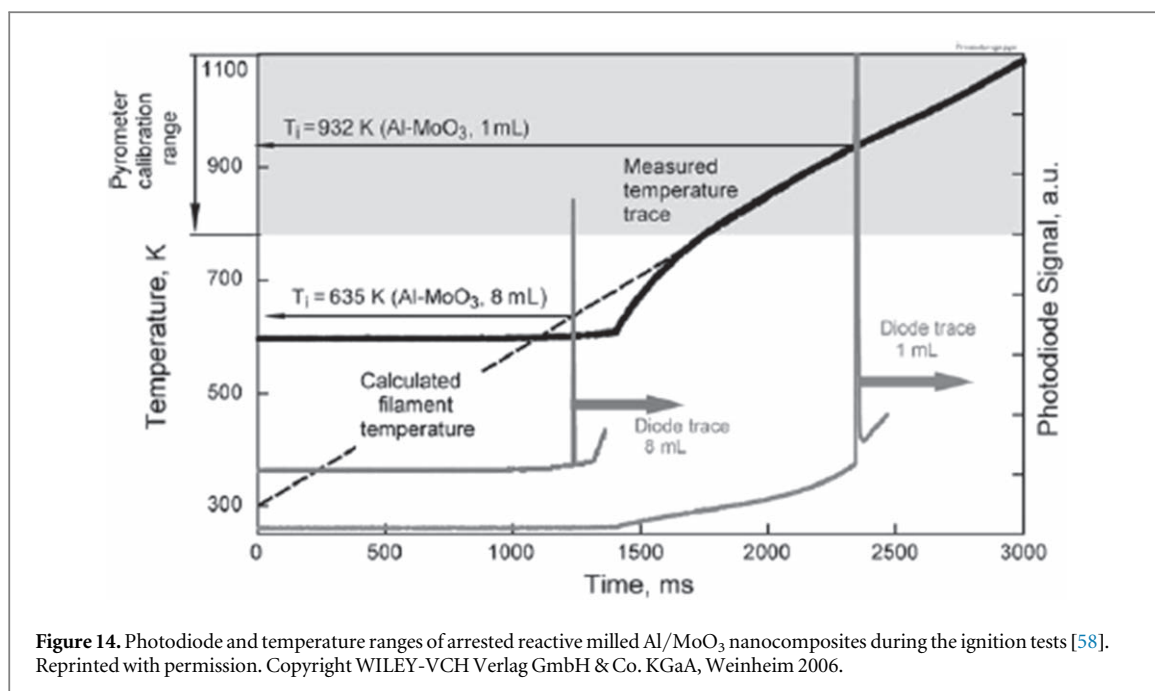


Figure 14. Photodiode and temperature ranges of arrested reactive milled Al/MoO₃ nanocomposites during the ignition tests [58]. Reprinted with permission. Copyright WILEY-VCH Verlag GmbH & Co. KGaA, Weinheim 2006.

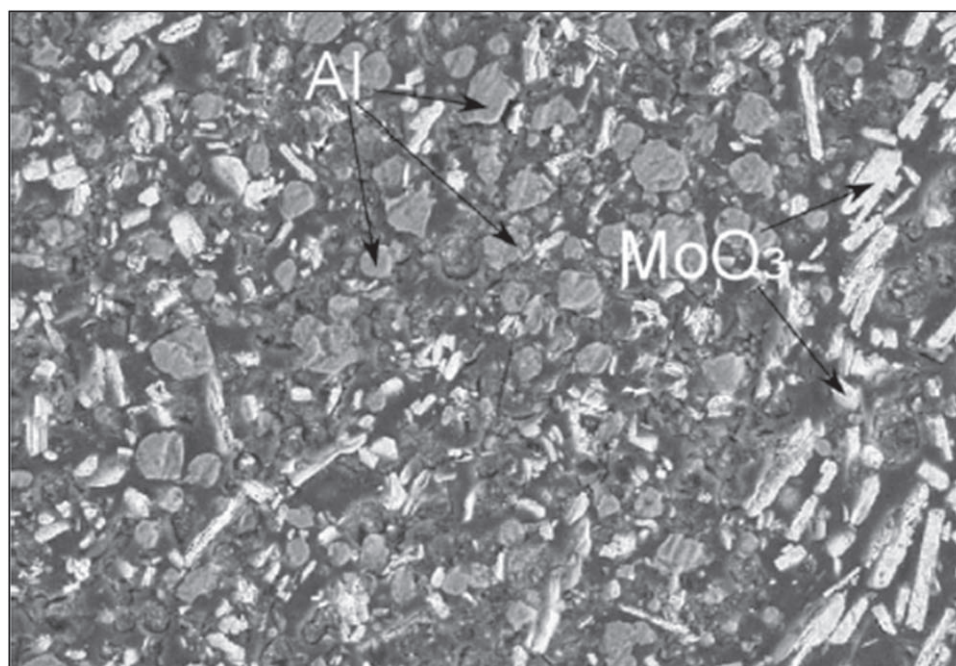


Figure 15. Backscattered electron (BSE)-SEM images of particle cross section of mixture of Al, MoO₃ powders [58]. Reprinted with permission. Copyright WILEY-VCH Verlag GmbH & Co. KGaA, Weinheim 2006.

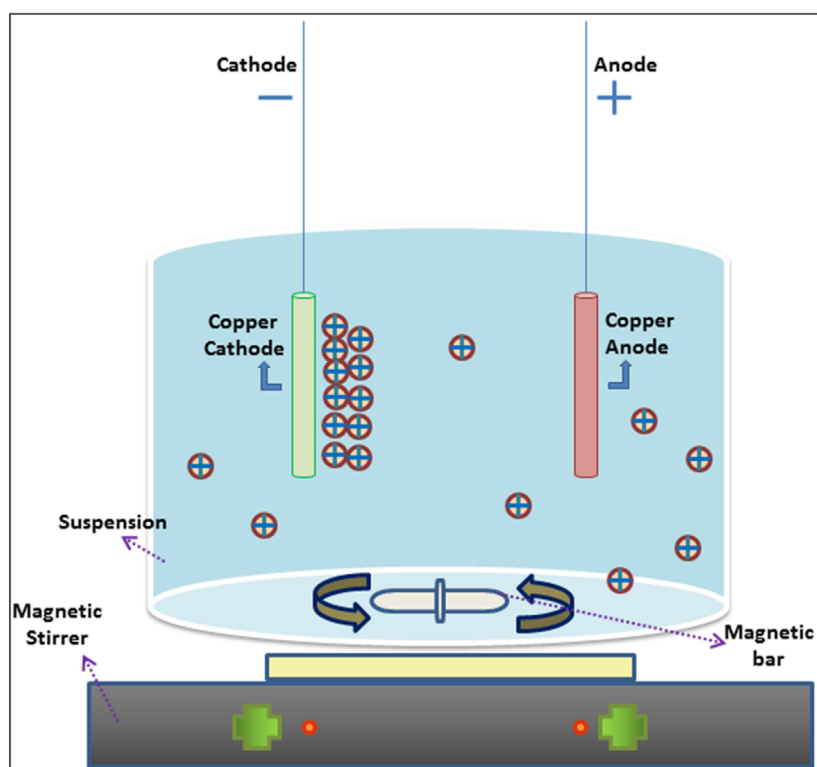
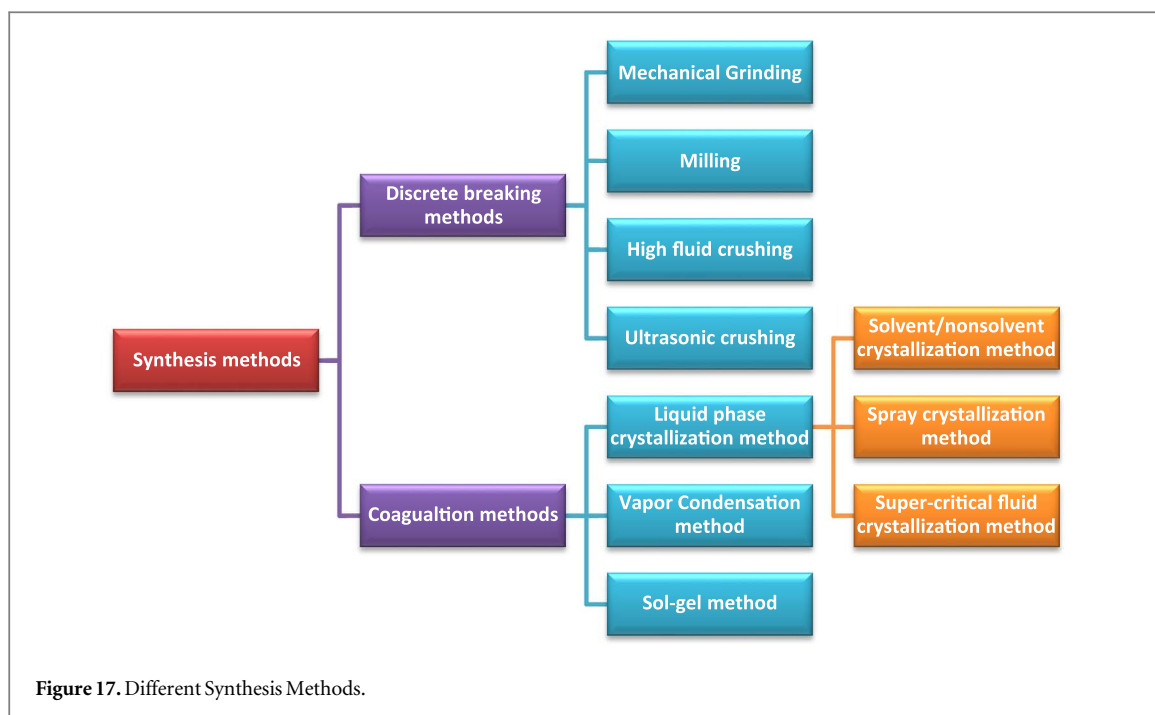


Figure 16. Schematic of Electrophoretic Deposition Setup [83]. Reprinted with permission. Copyright Elsevier B.V. 2013.



combustion properties of the Si/CuO based energetic systems produced by Electrophoretic deposition method [31]. The heat release value i.e., 244.3 kJ kg^{-1} was highest when the equivalence ratio was 1.0.

3.5. Solvent—non-solvent crystallization method

Comparing with the other few techniques available (figure 17) [84], this method has many advantages, like low cost, easy control over the process, simple crystallization principle, low operating temperature and wet state. Many NEMs prepared by this technique find application in slapper detonator and various other explosive devices. The liquid phase crystallization theory is the theoretical base for solvent/non-solvent process for the preparation of NEM. The solution has three different regions and three different states due to dissimilar concentrations during certain temperature and pressure conditions: unstable region, metastable region, stable region and supersaturated state, saturated state, unsaturated state. Making the solution attain state of super-saturation and nucleate swiftly in a very little time by combining non-solvent or weak solvent (commonly called non-solvent) and energetic material solution (liquid) strongly and quickly under precise conditions, is the key in making of NEM with solvent/non-solvent method. Nano scale energetic particles are prepared [84] by keeping under control the crystal nucleation and growth process and restraining the growth speed of crystal nuclei. Using this technique, a novel nanoenergetic composite was synthesized by coating Al/CuO with nano potassium perchlorate (KClO_4) and was found to have three times the burning rate of conventional compounds [85].

3.6. Powder mixing or mechanical/ultrasonic mixing

The ease of availability of n-Al powders enables them to be used widely for most of the metal-based reactive nanomaterials by utilizing simple powder mixing method. By means of commercially accessible ultrasonic cell disruptors or high intensity ultrasonic actuators the mixing is stereotypically carried out. In the lab assessments it is comparatively effective whereas the processing of large batches by ultrasonic mixing of nanopowders is very hard to scale up and may cause poor quality of mixing. Lately, nanothermites were synthesized by mixing the Fe_2O_3 and Al nanopowders through the rapid expansion of a supercritical dispersion (RESD) technique. Relative to the conventional ultrasonic mixing a much better mixing was accomplished. The RESD method is well-matched for continuous operation than ultrasonic mixing [41], in addition to giving a better mixing quality.

3.7. Self-assembly

For preparing reactive nanocomposite compositions with functionalized nanosized oxide particles and starting with nanosized aluminum powder, the self-assembly [62] methodology was taken into consideration. The metal particles were set over the outside surface area of oxide nanorods or in the ordered pore structure of the mesoporous oxidants in composites to create ordered assemblies. For instance, in an Al–CuO system, the self-assembly was attained with initial functionalization of CuO nanorods by using poly(4)-vinyl pyridine (P4VP), a monofunctional polymer. The nanorods gets ordered within the material since Al nanoparticles hold on to the functionalized nanorods. Better hold on the material properties along with the better reaction rates in practical

Table 7. Thermal behavior Al/CuO nanothermites with variation in the binder contents [89]. Reprinted with permission. Copyright John Wiley and Sons 2019.

| Binder content [wt %] | First exothermic peak (s) [°C] | Second exothermic peak (s) [°C] | Heat release [J g ⁻¹] |
|-----------------------|--------------------------------|---------------------------------|-----------------------------------|
| 10 | 364.8 | 622.5 | 292.6 |
| 15 | 372.8 | 620.4 | 245.3 |
| 20 | 364.8, 380.9 | 616.4 | 189.4 |
| 25 | 348.7, 372.8, 434.8 | 616.4 | 164.3 |

applications render the ordered nanocomposites more appealing compared to others. The inadequacies of this technique comprises of the high price of customized oxides, the existence of functionalizing agents that are usually responsible for reducing the energy density in energetic formulation, and the intrinsically high porosity of the materials [41, 62] produced.

3.8. Additive manufacturing: 3D printing

A printable reactive ink consisting of micron (75 micron sieve) and nanoscale aluminum (80 nm) solid inclusions based on the fluoro-polymer (THV-a polymer of tetrafluoroethylene, hexafluoropropylene and vinylidene fluoride) was created with its rheology suitably altered for direct-write assembly. Using usual pen type technique [86] the reactive inks were printed. Shen *et al* formulated a colloidal ink comprising of 90 wt% Al-CuO and the remaining 10 wt % of polymers like polystyrene, nitrocellulose and hydroxy propyl methyl cellulose (HPMC) to ease the fabrication process of high density reactive composites without hampering the combustion behavior and mechanical strength of the nanothermite [87]. Similarly, Wang *et al* used the direct ink writing (DIW) methodology and developed ink containing 10 wt% hybrid polymer of HPMC and polyvinylidene fluoride (PVDF) and 90 wt % nanothermite Al/CuO (Al = ~85 nm, CuO = ~40 nm). The ability of DIW technique to build structures with such high particle loading without the loss of mechanical strength along with the ease of adjustment of equivalence ratio, burn rate and rate of energy release has been drawing a lot of attention [88]. Mao *et al* [89] introduced a formula for new Al/CuO nanothermite ink that surpasses the existing limits and shortcomings of Al/CuO thermite and Direct-Ink-Writing (DIW). The presence of binder, F2311, helps in formulating hydrothermal inks with sound rheology shear-thinning properties, which proves to be useful in achieving the 3D printing of Al/CuO nanothermite. The printed patterns with loading as high as 75–90 wt% nanothermite are capable of attaining adjustable burn rates varying from 32 mm s⁻¹ to 352 mm s⁻¹. It is reported that the heat released increases with the loading of nanothermite (table 7) [89]. The competence of this method to achieve high resolution and precise patterns of nanothermite, makes it appropriate for different applications in micro energetic device with boosted combustion performance (figure 18) [89]. For 3D printing, this new strategy can very well be used with other nanothermite inks. Westphal *et al* have effectively deposited nanothermites like Al/CuO and Al/Bi₂O₃ on silicon substrate by inkjet printing and studied the effects of confinement and controllable fracturing performance that is generally employed in the electromechanical system security [90].

In addition, Murray *et al* proved that nAl (80 nm)/CuO (50 nm) nanothermite [91] can be successfully fabricated by reactive inkjet printing with improved safety, security and shelf stability. According to the high speed thermal imaging results, a difference of ~200 K prevailed between the maximum reaction temperature of samples printed with the dual nozzle and a single nozzle technique. Though wide range of energetic materials can be synthesized using this method, the lack of bulk characterization techniques opens up opportunities for researchers to work on providing solutions to this problem in the future developments.

4. Characteristics of nanoenergetic materials

4.1. Heat of reaction

Occurring at a constant pressure, the variation in the enthalpy of a chemical reaction or the difference in the heat of formation of the reactants and products is called as the heat of reaction or enthalpy of reaction. It is used for calculating the energy per mole either produced or released in a reaction. Table 8 shows the values of heat of reaction for some of the Al-based nanothermites [39, 45, 92, 93].

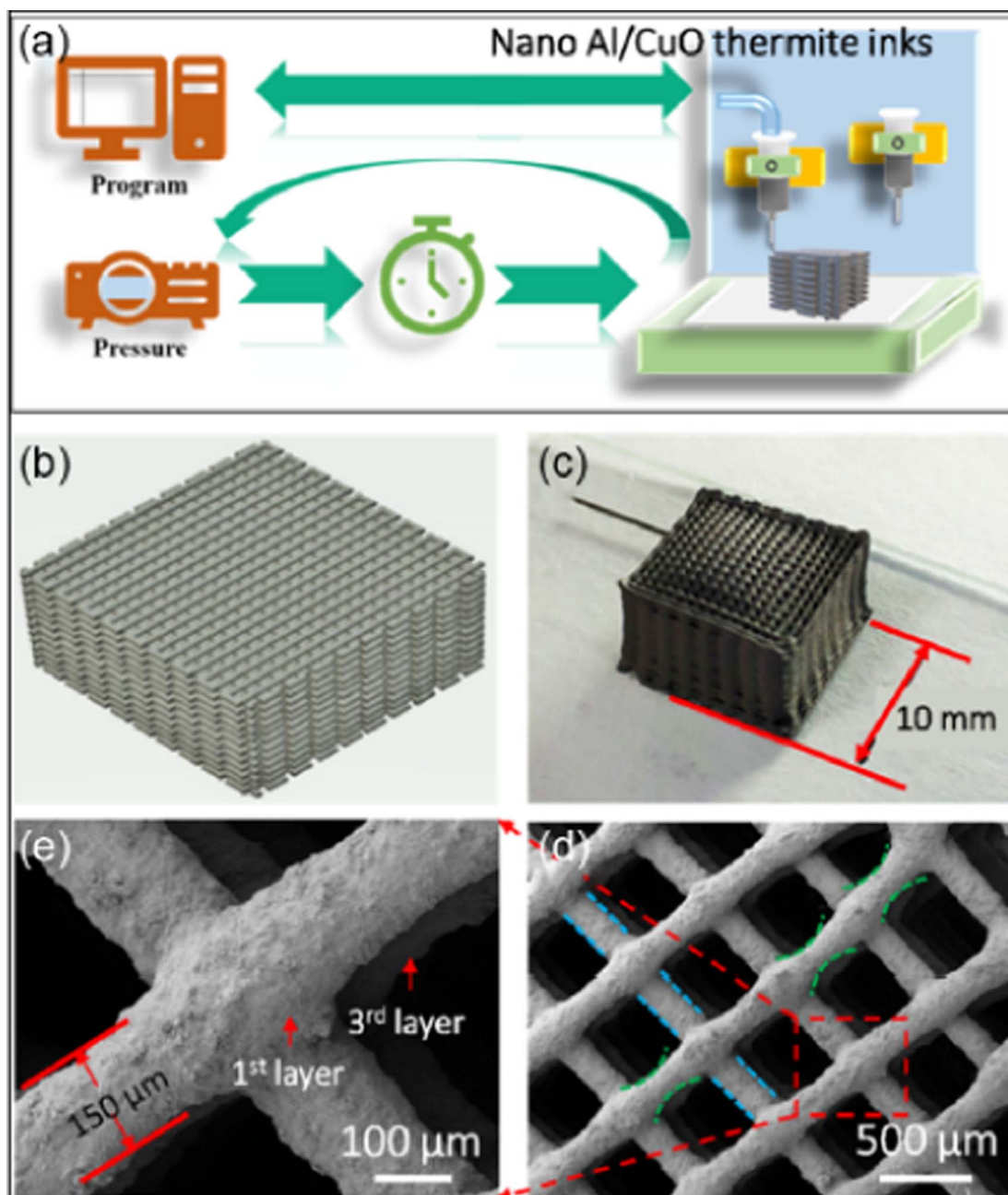


Figure 18. Al/CuO nanothermite by DIW 3D printing, (a) Schematic representation displaying the 3D printing, (b) Simulation pattern of 3D pattern configuration, (c) Image of Al/CuO nanothermite with 3D multilayer grid (cubic), (d) Magnified image (50X) of finely printed micro-architecture [89]. Reprinted with permission. Copyright WILEY-VCH Verlag GmbH & Co. KGaA, Weinheim, 2019.

Table 8. Heat of reaction for nanocomposites [39]. Reprinted with permission. Copyright Elsevier 2005.

| Chemical Reactions | Heat of reaction [kJ mol ⁻¹] | Adiabatic Temperature [K] |
|---|--|---------------------------|
| $2\text{Al} + 3\text{CuO} \rightarrow \text{Al}_2\text{O}_3 + 3\text{Cu}$ | -1186.6 | 2843 |
| $2\text{Al} + \text{MoO}_3 \rightarrow \text{Al}_2\text{O}_3 + \text{Mo}$ | -915.1 | 3820 |
| $2\text{Al} + \text{WO}_3 \rightarrow \text{Al}_2\text{O}_3 + \text{W}$ | -851.0 | 3476 |
| $2\text{Al} + \text{Fe}_2\text{O}_3 \rightarrow \text{Al}_2\text{O}_3 + 2\text{Fe}$ | -839.3 | 3135 |

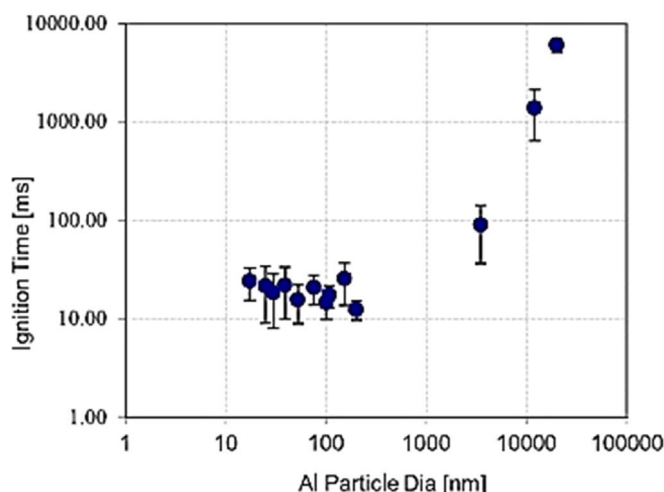


Figure 19. Ignition time of Al/MoO₃ as function of particle size [52, 67]. Reprinted with permission from Ref [67]. Copyright Elsevier Inc. 2004.

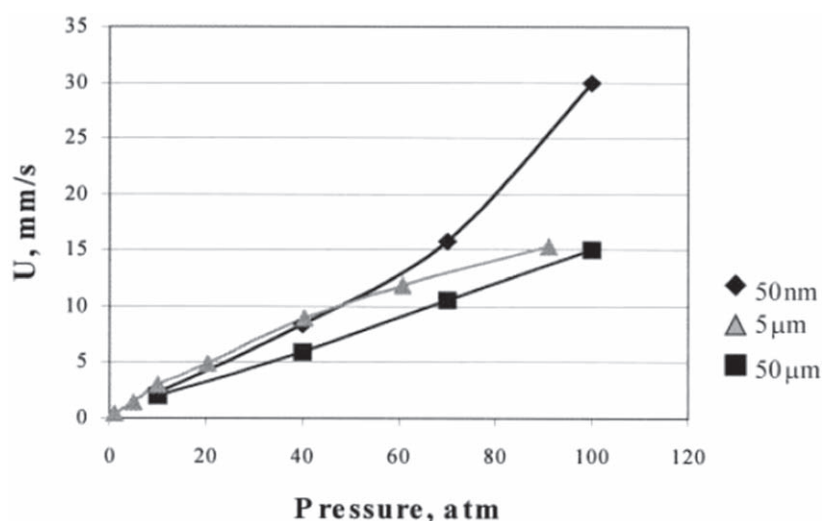


Figure 20. Burn rate as function of pressure of RDX monopropellant with particle size of 50 μm , 5 μm and 50 nm [98]. Reprinted with permission. Copyright WILEY-VCH Verlag GmbH & Co. KGaA, Weinheim 2004.

4.2. Ignition time

The ignition time is the time taken by the hot gas to come in contact with the propellant and cause the emission of light [94]. It is reported that the reduction in the fuel and oxidizer particles size reduces the diffusion distance between them thus increasing their intermixing and reaction rates and leading to less ignition times. The effect of particle diameter variation on the ignition time has been depicted in figure 19 [52, 67].

4.3. Ignition temperature

The ignition temperature is the temperature at which the energetic material combusts. It is another important facet of nano-thermite characterization in determining the suitability of the thermite for a particular application. This property is influenced by the particles size of the constituents of the thermite [95]. The reduction of size of Al particles in Al/MoO₃ thermite from 10–14 μm to 40 nm displays decrease in the ignition temperature from 955 °C to 458 °C respectively [48, 54].

4.4. Burning rate and pressure

It has been demonstrated by several researchers that faster burning rates can be achieved by using nano-sized particles instead of the micron-sized particles (figure 20) [96–99]. The burn rate—pressure relationship plays a vital role in determining the practicality of the nano thermite for a specific application. Mostly, as the pressure is

Table 9. Sb/KMnO₄ compositions in Perspex tubes (Open System) with their burning rates [101]. Reprinted with permission. Copyright Elsevier 1986.

| Sb particle size (μm) | % Sb | Burning Rate (mm s^{-1}) | |
|------------------------------------|------|-------------------------------------|---------------|
| | | Perspex | Aluminum |
| <8 | 30 | 2.7 ± 0.1 | 7.8 ± 0.1 |
| <8 | 40 | 2.7 ± 0.1 | 8.4 ± 0.1 |
| <8 | 50 | 2.7 ± 0.1 | 9.9 ± 0.2 |
| <53 | 30 | 1.3 ± 0.1 | 2.1 ± 0.1 |
| <53 | 35 | 1.6 ± 0.1 | 2.5 ± 0.1 |
| <53 | 50 | 2.9 ± 0.1 | |

elevated or reduced the burn rate increases or decreases. Also, temperature of the propellant has great influence on burn rate and as temperature increases it increases and as temperature decreases it decreases. All other parameters being same, the calorific value of the propellant influences the burn rate.

The Vieille's Law [21, 100] i.e. the exponential form of burn - rate law, is given as:

$$r = aP_c^n. \quad (3)$$

where,

r = burn rate (largely depends on propellant's initial temperature and chamber pressure)

a = coefficient that rely on the propellant's initial temperature (usually, $a = 0.002$ to 0.05)

P_c = pressure of the chamber

n = pressure index or exponent (function of propellant formulation)

Burning rate can be changed by altering the fuel/oxidant ratio or the particle size of the fuel (table 9) [101].

4.5. Lower impact sensitivity (impact, friction, electrostatic discharge)

Nanoscale thermites can be sensitive to both shock and impact or one of the two based on the metal oxide as compared to the thermites on micron-scale that are typically rather insensitive to shock and impact. The impact sensitivity can be classified into 4 classes: Insensitive (>40 J), Moderately sensitive ($35\text{--}40$ J), Sensitive ($4\text{--}35$ J), Very sensitive (<4 J) whereas the friction sensitivities are classified as: Insensitive (>360 N), Moderately sensitive ($80\text{--}360$ N), Sensitive ($10\text{--}80$ N), Very sensitive (<10 N) [54].

4.6. Specific impulse (I_{sp})

The foremost vital single ballistic property for rocket propellants [21] is the Specific impulse (I_{sp}). This property is very crucial in determining the mass of propellant needed to suffice the ballistic requirements and is expressed as the thrust per unit weight flow rate of propellant (w). I_{sp} of a propellant can be determined using equation (4).

$$I_{sp} = \frac{F}{w}. \quad (4)$$

where

F = thrust; w = weight flow rate.

5. Applications

5.1. Nanoenergetic gas generators (NGG), microthrusters and micropropulsion system, microelectromechanical systems (MEMS), microactuators

As per the intensive study done by Martirosyan *et al* the velocity of detonation of Al/Bi₂O₃ reached up to 2500 m s^{-1} whereas the minimum activation energy of approximately 150 kJ/mol , for Al/I₂O₅ system makes both the nanothermites suitable for applications as NGG [42]. Moreover the pressure impulses ($\sim 11 \text{ MPa}$) and higher values of energy densities render their application in microthrusters [100, 102] and micropropulsion systems. When compared with the hexane milling, the self-assembled nanoenergetic materials Al/Bi₂O₃ and Al/I₂O₅, displays elevation in the pressure discharge. Minimal quantities as low as 2 to 10 mg of manufactured nanoenergetic composites utilized in microthrusters are capable of producing a force ranging between 0.002 N to 0.6 N . For instance, 6000 N force can be generated by a group of $10,000$ microthrusters on a $0.5 \times 0.5 \text{ m}$ surface. Nanoenergetic composites also find applications in Microelectromechanical Systems (MEMS) [43, 45]. Table 10 shows the trend in the synthesis and development of novel energetic materials.

Table 10. Trends in the synthesis methods of novel energetic materials.

| Nano energetic composite | Synthesis method | Characterization techniques and properties examined | Results | References |
|--|--|---|---|-----------------------------|
| Al/PTFE, Al/PTFE/AP | Magnetic stirring and Crystallization | Energy and pressure output, Combustion properties | Energy Output: Pure Al/PTFE = 2019 J g ⁻¹ , Al/PTFE/AP (9 wt%) = 8863 J g ⁻¹ Pressurization rate: Pure Al/PTFE = 29.3 MPa ms ⁻¹ Al/PTFE/AP (9 wt%) = 340 MPa/ms Burn rate: Pure Al/PTFE = 260 m s ⁻¹ Al/PTFE/AP (9 wt%) = 1626 m s ⁻¹ | Wang <i>et al</i> [68] 2020 |
| Nano Si/CuO | Facile Electrophoretic deposition | Exothermic behaviors and Electrophoretic deposition dynamics XRD,SEM,EDS | The heat release of 259.9 kJ kg ⁻¹ was found to be highest at equivalence ratio of 1.0 as compared to the other ratios ($\phi = 0.5, 1.5, 2.0$). | Wang <i>et al</i> [31] 2019 |
| Al/CuO | Direct Ink Writing (DIW) 3D Printing | Thermal behavior | High ignition temperature and low combustion rate. The loading of nanothermite is up to 90 wt.%, and the highest value of burning rate obtained in the study for is 352 mm s ⁻¹ . | Mao <i>et al</i> [89] 2019 |
| Superfine RDX/Al composite (mass ratio of 70/30) | Mechanical ball-milling method | Activation energy, Thermal Sensitivity SEM, XPS,TGA,DSC, DSC-FTIR | Activation energy value of RDX in composite reduced to 70.8 kJ mol ⁻¹ and compared with the superfine RDX (119.6 kJ mol ⁻¹) Increase in the thermal sensitivity of the superfine RDX/Al | Xiao <i>et al</i> [16] 2018 |
| CL20 embedded with CuO/Al core/shell nanothermite arrays. | Facile dissolution-recrystallization | heat release characteristics (DSC) combustion phenomenon (Open burn tests) | Rise in milling time decreases the decomposition temperature Improved heat release properties with an increased total heat of reaction and an 18.2% subsided activation energy of integrated CL20. Displays a favorable burning behavior with a violent and steady combustion flame | Zhu <i>et al</i> [70] 2018 |
| Ternary mixtures KClO ₄ @Al/CuO | Solvent/non-solvent synthetic approach | Electrical ignition test, pressure cell test | Higher burning speeds Faster energy release velocity due to the decreased mass transfer distance and the rise of effect contact surface area of reactants | Yang <i>et al</i> [85] 2017 |
| Al/Bi ₂ O ₃ /P4VP (poly-4-vinylpyridine) | Self-assembly | Pressure discharge properties | The pressurization rates and peak pressures of Al/Bi ₂ O ₃ /P4VP and Al/Bi ₂ O ₃ /OA were 5590 kPa, 13.976 GPa s ⁻¹ and 4858 kPa, 12.146 GPa s ⁻¹ , respectively, better than those of Al/Bi ₂ O ₃ (4559 kPa, 11.397 GPa s ⁻¹). | Wang <i>et al</i> [62] 2017 |
| Al/Bi ₂ O ₃ /OA (Oleic acid) | | | | |

Table 10. (Continued.)

| Nano energetic composite | Synthesis method | Characterization techniques and properties examined | Results | References |
|--|---|--|--|-----------------------------------|
| Al/CuO Nanostructured energetic material | combination of a solution chemistry method and electrophoretic deposition | Thermal analysis | NEM had lowered the apparent activation energy for the solid state exothermic reaction, signifying the superior structural design | Zhou <i>et al</i> [103] 2016 |
| Ammonium perchlorate/Graphene oxide (AP/GO) | Recrystallization method/(fast crash) | Combustion behavior | 15% surge in the burning rate at a pressure of 80 atm | Memon <i>et al</i> [104] 2016 |
| Al/CuO and Al/MoO ₃ | mixing of powders by sonication | Dynamic pressure, linear propagation rates, and spectral emission, were measured | lowered the decomposition temperature of AP Nano Al/nano CuO ($\phi = 1.1$) | Weismiller <i>et al</i> [55] 2011 |
| Al/Teflon | — | Ultrafast IR spectroscopy to study the reactions between flash-heated Al nano-particles and Teflon ^{AF} | Linear burning rate = 980 m s ⁻¹ , Mass burning rate = 3.8 kg s ⁻¹ , Energetic mass burning rate = 3.1 kg s ⁻¹ , Nano Al/nano MoO₃ ($\phi = 1.4$) Linear burning rate = 680 m s ⁻¹ , Mass burning rate = 2.0 kg s ⁻¹ , Energetic mass burning rate = 1.4 kg s ⁻¹ , The reactions of Al with CF ₂ and CF ₃ have the same apparent rate, thus it proved possible to explain the Al + Teflon ^{AF} chemistry with the slower processes involving | Zamkov <i>et al</i> [69] 2007 |
| Teflon: a copolymer of tetrafluoroethylene (TFE) and 2,2-bis(trifluoromethyl)-4,5-difluoro-1,3-dioxole (dioxole), the mass ratio of Teflon ^{AF} /Al = 4.6 | | | Al + CF ₂ or CF ₃ and the faster involving Al + CFO. | |
| | | | The reactions with CFO were >10 times faster than reactions with CF ₂ or CF ₃ . | |

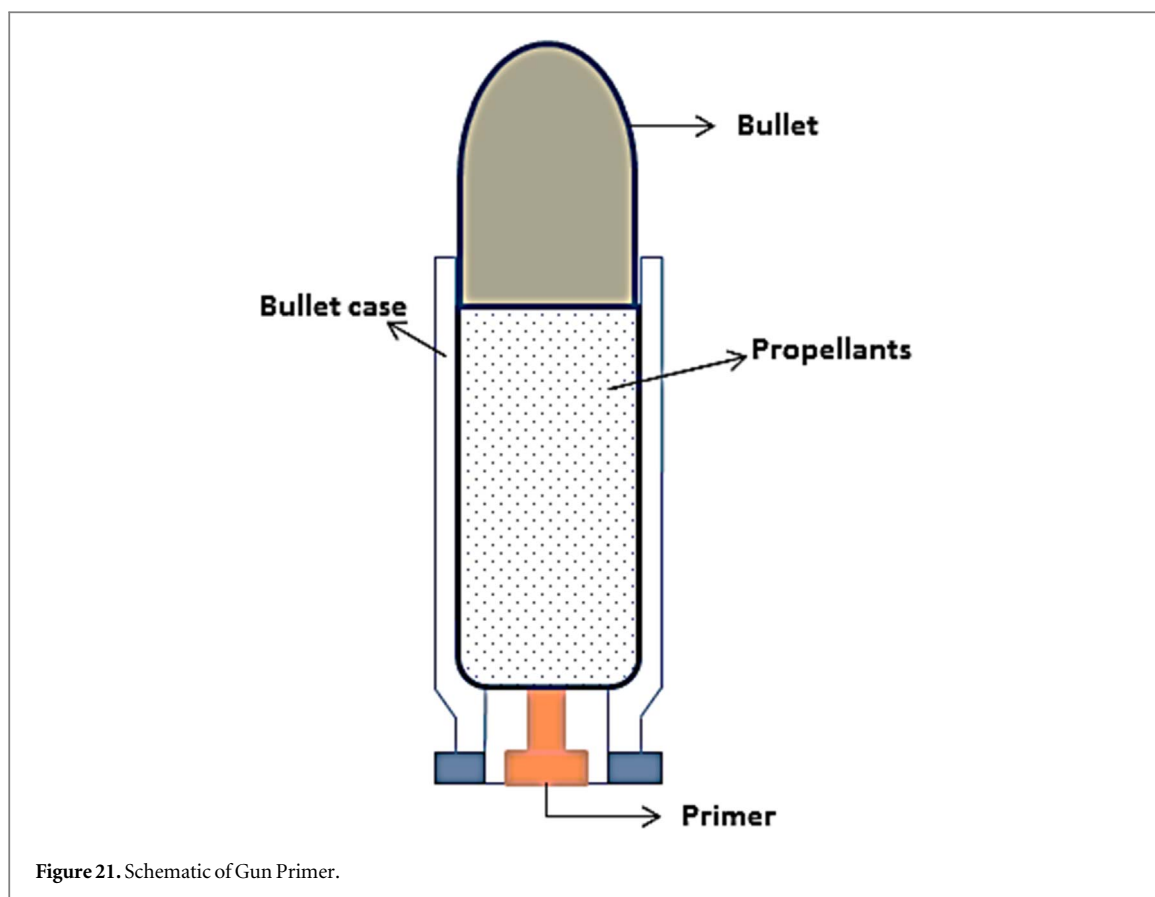


Figure 21. Schematic of Gun Primer.

5.2. Gun primers and electric matches

By varying size of particles or by usage of different nanoscale materials and varying the ratio of fuel to oxidizer of the composite, the super-thermite materials are made to be more sensitive towards thermal stimuli like resistive heating thus rendering them capable of replacing the lead-containing compounds in the electric matches/igniters as well as non-toxic gun or electric primers (figure 21) [54, 66, 105, 106].

5.3. Biocidal agent

Sullivan *et al* examined the reaction and ignition of Al/AgIO₃ thermites for plausible usage in various biocidal applications. Its ignition temperature of the Al/AgIO₃ was found to be between 1175 K to 1255 K whereas the pressurization rate outperforms that of Al/CuO [92]. Ivan Davila [107] composed a ternary-thermite system, which acted as NGG, having composition 10/75/15 wt % of I₂O₅/Ag₂O/Al. The highly pathogenic microorganisms or bacteria are destroyed by the mixtures ability imparted to it by the production of biocidal gases from this composition. In this study, due to the production of a strong biocidal environment by the gaseous silver and iodine produced from NGG combustion, the living strain cells of *Escherichia coli* (*E. coli*) K-12 were destroyed. Likewise, the potent biocidal properties of Iodine-containing gases have been employed by Wang *et al* and successfully prepared a reactive ternary composite system of Mg-B-I₂ by mechanical milling of powders in two steps. Such reactive composites have potential to be used in munitions that can be used against biological weapons [108].

5.4. Molecular delivery applications

Patel *et al* ignited Co₃O₄/nAl and Co₃O₄ (calcined at 400 °C)/nAl nanoenergetic composites and reported the peak pressure/pressurization rates [109] and combustion front-wave speed. The heat of reaction was recorded to be 1.02 kJ g⁻¹ for calcined Co₃O₄-400/nAl and 0.96 kJ g⁻¹ for Co₃O₄/nAl nanoenergetic systems. The Co₃O₄-400/nAl and Co₃O₄/nAl nanoenergetic composite propagated at a maximum flame-front speed of 830 ± 75 m s⁻¹ and 781 ± 50 m s⁻¹ respectively. The maximum peak pressure, nearly similar to the CuO-based nanoenergetic system, was obtained at an equivalence ratio of 1.6, but due to low gas generation during the combustion process the maximum pressurization rate with Co₃O₄/nAl (0.47 ± 0.1 MPa μs⁻¹) was much lower to that of CuO/nAl nanoenergetics. The Co₃O₄/nAl nanoenergetic system can create pressurization rate from ~0.03 to 0.19 MPa μs⁻¹ whereas mild peak pressure ranging from 12.6 ± 1 MPa to 20 ± 2 MPa that attributes

to the low gas generation characteristics, and thus find application in low intensity pressure-pulse based microporation of soft matters such as bacterial cells without analysis [109].

6. Conclusion

Comprehensive analysis of various fabrication approaches and research accomplishments so far has been presented in the review paper. The reduction in size of particles to nanometric scale and its further incorporation to prepare nanoenergetic composites have elevated the potential of conventional energetic compounds and led to development of novel thermite systems. Nanothermites are a promising candidate for developing advanced energetic systems with desirable high energy densities, faster energy release rates, lower impact sensitivity, high burning rates, high specific impulse and so on for applications in Nanoenergetic Gas Generators (NGG), microthrusters and micropropulsion system, microelectromechanical systems (MEMS). Al-based metastable interstitial composites have been extensively explored by researchers by employing the traditional synthesis techniques. However, nowadays, other metallic fuels like Si, Sb, Mn, Zr, and advanced synthesis processes like Direct Ink Writing (DIW) 3D printing have grabbed the attention of the researchers. Despite the advantages of the nanothermite systems, the safety and security issues hinders the usage of nanoenergetic materials to a certain extent. Thus, a significant work can be done to broaden the scope of nanoenergetic materials for diverse future applications.

Acknowledgments

The authors are thankful to Dr. C. P. Ramanarayanan, Vice-Chancellor of DIAT (DU), for the lab facilities, motivation, and support. The authors are thankful to all group members at DIAT (DU), for the technical support provided during preparation of the manuscript. The authors are thankful to the anonymous Reviewers and the Editor, for improving the quality of revised manuscript by their valuable suggestions and comments.

ORCID iDs

Balasubramanian Kandasubramanian  <https://orcid.org/0000-0003-4257-8807>

References

- [1] Zhou X, Torabi M, Lu J, Shen R and Zhang K 2014 Nanostructured energetic composites: synthesis, ignition/combustion modeling, and applications *ACS Appl. Mater. Interfaces* **6** 3058–3074
- [2] Fried L E, Manaa M R, Pagoria P F and Simpson R L 2001 Design and synthesis of energetic materials *Annu. Rev. Mater. Res.* **31** 291–321
- [3] Kelly J 2005 *Gunpowder: Alchemy, Bombards, and Pyrotechnics: the History of the Explosive that Changed the World* (New York: Basic Books)
- [4] Behrens R and Swanson R 2007 A new paradigm for R&D to implement new energetic materials in munitions 2007 *Insensitive Munitions & Energetic Materials Technology Symp.* (National Defense Industrial Association (NDIA)) p 13
- [5] Anderson K J 1989 Energetic materials, I: black powder, nitroglycerin, and dynamite *MRS Bull.* **14** 84–86
- [6] Anderson K J 1989 Energetic materials: II. TNT and other military explosives *MRS Bull.* **14** 63–64
- [7] Spear R J and Wilson W S 1984 Recent approaches to the synthesis of high explosive and energetic materials: a review *J. Energetic Mater.* **2** 61–149
- [8] Adams G F and Shaw R W 1992 Chemical reactions in energetic materials *Annu. Rev. Phys. Chem.* **43** 311–40
- [9] Dedgaonkar V G, Navle P B and Shrotri P G 1996 Radiation curing of AP/HTPB-based energetic composites: I. Effect on physico-mechanical properties *Propellants Explos. Pyrotech.* **21** 303–6
- [10] Isbell R A and Brewster M Q 1998 Optical properties of energetic materials: RDX, HMX, AP, NC/NG, and HTPB *Propellants Explos. Pyrotech.* **23** 218–24
- [11] Mellor A M et al 1988 Hazard initiation in solid rocket and gun propellants and explosives *Prog. Energy Combust. Sci.* **14** 213–44
- [12] Elbasuney S, Gaber Zaky M, Radwan M and Mostafa S F 2017 Stabilized super-thermite colloids: a new generation of advanced highly energetic materials *Appl. Surf. Sci.* **419** 328–36
- [13] Dlott D D 2006 Thinking big (and small) about energetic materials *Mater. Sci. Technol.* **22** 463–73
- [14] Kappagantula K and Pantoya M 2016 Fast-reacting nanocomposite energetic materials *Energetic Nanomaterials* (Amsterdam: Elsevier) pp 21–45
- [15] Wang Y, Song X, Song D, Liang L, An C and Wang J 2016 Synthesis, thermolysis, and sensitivities of HMX/NC energetic nanocomposites *J. Hazard. Mater.* **312** 73–83
- [16] Xiao L, Zhang Y, Wang X, Hao G, Liu J, Ke X, Chen T and Jiang W 2018 Preparation of a superfine RDX/Al composite as an energetic material by mechanical ball-milling method and the study of its thermal properties *RSC Adv.* **8** 38047–55
- [17] Geetha M, Nair U R, Sarwade D B, Gore G M, Asthana S N and Singh H 2003 Studies on CL-20: the most powerful high energy material *J. Therm. Anal. Calorim.* **73** 913–22
- [18] Chaturvedi S and Dave P N 2019 Solid propellants: AP/HTPB composite propellants *Arabian J. Chem.* **12** 2061–8
- [19] Jain S, Khire V H and Kandasubramanian B 2019 Barium titanate: a novel perovskite oxide burning rate modifier for HTPB/AP/Al based composite propellant formulations *Propellants Explos. Pyrotech.* **44** 505–12

- [20] Jain S, Gupta G, Kshirsagar D R, Khire V H and Kandasubramanian B 2019 Burning rate and other characteristics of strontium titanate (SrTiO_3) supplemented AP/HTPB/Al composite propellants *Defence Technology* **15** 313–8
- [21] Ashish J, Swaroop G and Balasubramanian K 2019 chapter 8 - Effect of ammonium perchlorate particle size on flow, ballistic, and mechanical properties of composite propellant *Nanomaterials in Rocket Propulsion Systems Micro and Nano Technologies* ed Q-L Yan et al (Amsterdam: Elsevier) pp 299–362
- [22] Paterson S and Davidson J M 1962 Detonation in Ammonium Nitrate *Nature* **195** 277–8
- [23] Rice S F and Simpson R L 1990 *The unusual stability of TATB (1,3,5-triamino-2,4,6-trinitrobenzene): a review of the scientific literature* UCRL-1R-103683 ON: DE91001078 Lawrence Livermore National Laboratory 1–22
- [24] Pagoria P F, Lee G S, Mitchell A R and Schmidt R D 2002 A review of energetic materials synthesis *Thermochim. Acta* **384** 187–204
- [25] Tillotson T M, Gash A E, Simpson R L, Hrubesh L W, Satcher J H and Poco J F 2001 Nanostructured energetic materials using sol-gel methodologies *J. Non-Cryst. Solids* **285** 338–45
- [26] Armstrong R W, Baschung B, Booth D W and Samirant M 2003 Enhanced propellant combustion with nanoparticles *Nano Lett.* **3** 253–5
- [27] Parks R L 1980 *Remote Handling: Blending of Energetic Materials* (OH (USA): Mound Facility, Miamisburg)
- [28] Kang X, Li C, Zheng Z and Cui X 2019 Facile preparation of micrometer KClO_4/Zr energetic composite particles with enhanced light radiation *Materials* **12** 199
- [29] Fischer S H and Grubelich M C 1998 *Theoretical energy release of thermites, intermetallics, and combustible metals* SAND-98-1176C; CONF-980728-ON: DE98005512 Sandia National Laboratories 1–56
- [30] Brown M E, Taylor S J and Tribelhorn M J 1998 Fuel—oxidant particle contact in binary pyrotechnic reactions *Propellants Explos. Pyrotech.* **23** 320–7
- [31] Wang Q, Xing B, Guo X, Bao H, Wang Y, Li A, Xu P and Li X 2019 Facile preparation of Si/CuO energetic materials by electrophoretic deposition and their exothermic studies *Vacuum* **167** 244–8
- [32] Huang S, Deng S, Jiang Y, Zhao J and Zheng X 2017 Electroless deposition and ignition properties of Si/ Fe_2O_3 core/shell nanothermites *ACS Omega* **2** 3596–600
- [33] Apperson S, Shende R V, Subramanian S, Tappmeyer D, Gangopadhyay S, Chen Z, Gangopadhyay K, Redner P, Nicholich S and Kapoor D 2007 Generation of fast propagating combustion and shock waves with copper oxide/aluminum nanothermite composites *Appl. Phys. Lett.* **91** 243109
- [34] Kim K J, Cho M H and Kim S H 2018 Effect of aluminum micro- and nanoparticles on ignition and combustion properties of energetic composites for interfacial bonding of metallic substrates *Combust. Flame* **197** 319–27
- [35] Menon L, Patibandla S, Kanchibotla B, Shkuratov S, Aurongzeb D, Holtz M, Berg J, Yun J and Temkin H 2004 Ignition studies of AlOFe_2O_3 energetic nanocomposites *Appl. Phys. Lett.* **84** 4735–7
- [36] Durães L, Costa B F O, Santos R, Correia A, Campos J and Portugal A 2007 Fe_2O_3 /aluminum thermite reaction intermediate and final products characterization *Materials Science and Engineering: A* **465** 199–210
- [37] Patel V K, Kant R, choudhary A, Painuly M and Bhattacharya S 2019 Performance characterization of $\text{Bi}_2\text{O}_3/\text{Al}$ nanoenergetics blasted micro-forming system *Defence Technology* **15** 98–105
- [38] Geeson J, Staley C, Bok S, Thiruvengadathan R, Gangopadhyay K and Gangopadhyay S 2017 Graphene-based Al- Bi_2O_3 nanoenergetic films by electrophoretic deposition *2017 IEEE 12th Nanotechnology Materials and Devices Conf. (NMDC) 2017 IEEE 12th Nanotechnology Materials and Devices Conf. (NMDC) (Singapore)* (IEEE) pp 58–9
- [39] Valliappan S, Swiatkiewicz J and Puszyński J A 2005 Reactivity of aluminum nanopowders with metal oxides *Powder Technol.* **156** 164–9
- [40] Bockmon B S, Pantoya M L, Son S F, Asay B W and Mang J T 2005 Combustion velocities and propagation mechanisms of metastable interstitial composites *J. Appl. Phys.* **98** 064903
- [41] Dreizin E L 2009 Metal-based reactive nanomaterials *Prog. Energy Combust. Sci.* **35** 141–67
- [42] Hobosyan M A and Martirosyan K S 2020 Novel nanoenergetic materials: emerging trends and applications *IEEE Nanotechnol. Mag.* **14** 30–6
- [43] Jiang Y et al 2018 Energetic performance of optically activated aluminum/graphene oxide composites *ACS Nano* **12** 11366–75
- [44] Dai J, Xu J, Wang F, Tai Y, Shen Y, Shen R and Ye Y 2018 Facile formation of nitrocellulose-coated Al/ Bi_2O_3 nanothermites with excellent energy output and improved electrostatic discharge safety *Mater. Des.* **143** 93–103
- [45] Rossi C, Zhang K, Esteve D, Alphonse P, Tailhades P and Vahlas C 2007 Nanoenergetic materials for MEMS: a review *J. Microelectromech. Syst.* **16** 919–31
- [46] Kasztankiewicz A, Gańczyk-Specjalska K, Zygmunt A, Cieślak K, Zakościelny B and Gołofit T Mar 2018 Application and properties of aluminum in rocket propellants and pyrotechnics *Journal of Elementology* **23** 321–31 11p
- [47] Bhattacharya S, Agarwal A K, Patel V K, Raja Gopalan T, Basu A K and Saha A 2019 Introduction to Nano-energetic Materials *Nano-Energetic Materials Energy, Environment, and Sustainability* ed S Bhattacharya et al (Singapore: Springer) pp 3–7
- [48] Pantoya M L and Granier J J 2005 Combustion behavior of highly energetic thermites: nano versus micron composites *Propellants Explos. Pyrotech.* **30** 53–62
- [49] Pantoya M L, Levitas V I, Granier J J and Henderson J B 2009 Effect of bulk density on reaction propagation in nanothermites and micron thermites *J. Propul. Power* **25** 465–70
- [50] Gibot P and Goetz V 2019 Aluminium/tin (IV) oxide thermite composite: sensitivities and reaction propagation *J. Energetic Mater.* **0** 1–14
- [51] Thiruvengadathan R, Belarde G M, Bezmelnitsyn A, Shub M, Balas-Hummers W, Gangopadhyay K and Gangopadhyay S 2012 Combustion characteristics of silicon-based nanoenergetic formulations with reduced electrostatic discharge sensitivity *Propellants Explos. Pyrotech.* **37** 359–72
- [52] Sundaram D, Yang V and Yetter R A 2017 Metal-based nanoenergetic materials: Synthesis, properties, and applications *Prog. Energy Combust. Sci.* **61** 293–365
- [53] Rossi C, Estève A and Vashishta P 2010 Nanoscale energetic materials *J. Phys. Chem. Solids* **2** 57–8
- [54] Piercey D G and Klapötke T M 2010 Nanoscale aluminum—metal oxide (Thermite) reactions for application in energetic materials *Cent. Eur. J. Energetic Mater.* **7** 115–29
- [55] Weismiller M R, Malchi J Y, Lee J G, Yetter R A and Foley T J 2011 Effects of fuel and oxidizer particle dimensions on the propagation of aluminum containing thermites *Proc. Combust. Inst.* **33** 1989–96
- [56] Zhang K, Rossi C, Ardila Rodriguez G A, Tenailleau C and Alphonse P 2007 Development of a nano-Al/CuO based energetic material on silicon substrate *Appl. Phys. Lett.* **91** 113117
- [57] Koch E and Knapp S 2019 Thermites—versatile materials *Prop., Explos., Pyrotech.* **44** 7–7

- [58] Umbrajkar S M, Schoenitz M and Dreizin E L 2006 Control of structural refinement and composition in Al-MoO₃ nanocomposites prepared by arrested reactive milling *Propellants Explos. Pyrotech.* **31** 382–9
- [59] Schefflan R, Kovenklioglu S, Kalyon D, Mezger M and Leng M 2006 Formation of aluminum nanoparticles upon condensation from vapor phase for energetic applications *J. Energetic Mater.* **24** 141–56
- [60] Ivanov Y F, Osmonoliev M N, Sedoi V S, Arkhipov V A, Bondarchuk S S, Vorozhtsov A B, Korotkikh A G and Kuznetsov V T 2003 Productions of ultra-fine powders and their use in high energetic compositions *Propellants Explos. Pyrotech.* **28** 319–33
- [61] Lerner M, Vorozhtsov A, Guseinov S and Storozhenko P 2014 Metal nanopowders production *Metal Nanopowders: Production, Characterization, and Energetic Applications* ed A Gromov and U Teipel (Weinheim, Germany: Wiley-VCH Verlag GmbH & Co. KGaA) pp 79–106
- [62] Wang Y, Yu H, Jiang Z and Guo L 2017 Improved pressure discharge property of surface modified Al/Bi₂O₃ composites *Russ. J. Appl. Chem.* **90** 1330–6
- [63] Chowdhury P S, Arya P R and Raha K 2007 Green synthesis of nanoscopic iron oxide particles: a potential oxidizer in nanoenergetics *Synthesis and Reactivity in Inorganic, Metal-Organic, and Nano-Metal Chemistry* **37** 447–51
- [64] Cheng J L, Hng H H, Ng H Y, Soon P C and Lee Y W 2010 Synthesis and characterization of self-assembled nanoenergetic Al-Fe₂O₃ thermite system *J. Phys. Chem. Solids* **71** 90–4
- [65] Sanders V E, Asay B W, Foley T J, Tappan B C, Pacheco A N and Son S F 2007 Reaction propagation of four nanoscale energetic composites (Al/MoO₃, Al/WO₃, Al/CuO, and Bi₂O₃) *J. Propul. Power* **23** 707–14
- [66] Glavier L, Taton G, Ducéré J-M, Baijot V, Pinon S, Calais T, Estève A, Djafari Rouhani M and Rossi C 2015 Nanoenergetics as pressure generator for nontoxic impact primers: comparison of Al/Bi₂O₃, Al/CuO, Al/MoO₃ nanothermites and Al/PTFE *Combust. Flame* **162** 1813–20
- [67] Granier J J and Pantoya M L 2004 Laser ignition of nanocomposite thermites *Combust. Flame* **138** 373–83
- [68] Wang J, Zhang L, Mao Y and Gong F 2020 An effective way to enhance energy output and combustion characteristics of Al/PTFE *Combust. Flame* **214** 419–25
- [69] Zamkov M A, Conner R W and Dlott D D 2007 Ultrafast chemistry of nanoenergetic materials studied by time-resolved infrared spectroscopy: aluminum nanoparticles in teflon *J. Phys. Chem. C* **111** 10278–84
- [70] Zhu Y, Zhou X, Xu J, Ma X, Ye Y, Yang G and Zhang K 2018 *In situ* preparation of explosive embedded CuO/Al/CL20 nanoenergetic composite with enhanced reactivity *Chem. Eng. J.* **354** 885–95
- [71] Manesh N A, Basu S and Kumar R 2010 Experimental flame speed in multi-layered nano-energetic materials *Combust. Flame* **157** 476–80
- [72] Petrantonio M, Rossi C, Salvagnac L, Conédéra V, Estève A, Tenaillieu C, Alphonse P and Chabal Y J 2010 Multilayered Al/CuO thermite formation by reactive magnetron sputtering: Nano versus micro *J. Appl. Phys.* **108** 084323
- [73] Ferguson J D, Buechler K J, Weimer A W and George S M 2005 SnO₂ atomic layer deposition on ZrO₂ and Al nanoparticles: pathway to enhanced thermite materials *Powder Technol.* **156** 154–63
- [74] Miziolek D A W 2002 Nanoenergetics: an emerging technology area of national importance *AMMTIAC* **6** 43–8
- [75] Rao B G, Mukherjee D and Reddy B M 2017 chapter 1 - Novel approaches for preparation of nanoparticles *Nanostructures for Novel Therapy Micro and Nano Technologies* ed D Fica and A M Grumezescu (Amsterdam: Elsevier) pp 1–36
- [76] Cervantes O G, Kuntz J D, Gash A E and Munir Z A 2010 Heat of combustion of tantalum–tungsten oxide thermite composites *Combust. Flame* **157** 2326–32
- [77] Kuntz J D, Cervantes O G, Gash A E and Munir Z A 2010 Tantalum–tungsten oxide thermite composites prepared by sol–gel synthesis and spark plasma sintering *Combust. Flame* **157** 1566–71
- [78] Ward T, Chen W, Schoenitz M, Dreizin E and Dave R 2005 Nano-composite energetic powders prepared by arrested reactive milling *43rd AIAA Aerospace Sciences Meeting and Exhibit 43rd AIAA Aerospace Sciences Meeting and Exhibit (Reno, Nevada)* (American Institute of Aeronautics and Astronautics)
- [79] Badiola C, Schoenitz M, Zhu X and Dreizin E L 2009 Nanocomposite thermite powders prepared by cryomilling *J. Alloys Compd.* **488** 386–91
- [80] Shen L-H, Li G-P, Yunjun L, Gao K, Chai C-P and Ge Z 2014 Preparation of Al/B/Fe₂O₃ nano-composite energetic materials by high energy ball milling *Guti Huojian Jishu/Journal of Solid Rocket Technology* **37** 233–7
- [81] Ke X, Zhou X, Hao G, Xiao L, Liu J and Jiang W 2017 Rapid fabrication of superhydrophobic Al/Fe₂O₃ nanothermite film with excellent energy-release characteristics and long-term storage stability *Appl. Surf. Sci.* **407** 137–44
- [82] Sullivan K T, Kuntz J D and Gash A E 2013 Fine patterning of thermites for mechanistic studies and microenergetic applications *IJEMCP* **12**
- [83] Singh B P, Jena B K, Bhattacharjee S and Besra L 2013 Development of oxidation and corrosion resistance hydrophobic graphene oxide-polymer composite coating on copper *Surf. Coat. Technol.* **232** 475–481
- [84] Zeng G, Zhao L, Zeng X and Qiao Z 2018 Preparation progress of micro/nano-energetic materials *IOP Conf. Ser.: Mater. Sci. Eng.* **382** 022030
- [85] Yang F, Kang X, Luo J, Yi Z and Tang Y 2017 Preparation of core-shell structure KClO₄@Al/CuO Nanoenergetic material and enhancement of thermal behavior *Sci. Rep.* **7** 1–9
- [86] Ruz-Nuglo F D and Groven L J 2018 3D printing and development of fluoropolymer based reactive inks *Adv. Eng. Mater.* **20** 1700390
- [87] Shen J, Wang H, Kline D J, Yang Y, Wang X, Rehwoldt M, Wu T, Holdren S and Zachariah M R 2020 Combustion of 3D printed 90 wt% loading reinforced nanothermite *Combust. Flame* **215** 86–92
- [88] Wang H, Shen J, Kline D J, Eckman N, Agrawal N R, Wu T, Wang P and Zachariah M R 2019 Direct writing of a 90 wt% particle loading nanothermite *Adv. Mater.* **31** 1806575
- [89] Mao Y, Zhong L, Zhou X, Zheng D, Zhang X, Duan T, Nie F, Gao B and Wang D 2019 3D printing of Micro-Architected Al/CuO-based nanothermite for enhanced combustion performance *Adv. Eng. Mater.* **21** 1900825
- [90] Westphal E R, Murray A K, McConnell M P, Fleck T J, Chiu G T-C, Rhoads J F, Gunduz I E and Son S F 2019 The effects of confinement on the fracturing performance of printed nanothermites *Prop., Explos., Pyrotech.* **44** 47–54
- [91] Murray A K, Isik T, Ortalan V, Gunduz I E, Son S F, Chiu G T-C and Rhoads J F 2017 Two-component additive manufacturing of nanothermite structures via reactive inkjet printing *J. Appl. Phys.* **122** 184901
- [92] Sullivan K T, Piekielek N W, Chowdhury S, Wu C, Zachariah M R and Johnson C E 2010 Ignition and combustion characteristics of nanoscale Al/AgIO₃: a potential energetic biocidal system *Combust. Sci. Technol.* **183** 285–302
- [93] Bohloul Z G 2013 *Synthesis, Characterization, and Application of Nanothermites for Joining* University of Waterloo
- [94] McAlevy R, Cowan P and Summerfield M 1960 The mechanism of ignition of composite solid propellants by hot gases *Solid Propellant Rocket Research* ed M Summerfield (New York: American Institute of Aeronautics and Astronautics)) 1

- [95] Egan G C, Mily E J, Maria J-P and Zachariah M R 2015 Probing the reaction dynamics of thermite nanolaminates *J. Phys. Chem. C* **119** 20401–8
- [96] Granier J J and Pantoya M L 2004 The effect of size distribution on burn rate in nanocomposite thermites: a probability density function study *Combust. Theor. Model.* **8** 555–65
- [97] Dokhan A, Price E, Sigman R and Seitzman J 2001 The effects of Al particle size on the burning rate and residual oxide in aluminized propellants 37th Joint Propulsion Conf. and Exhibit 37th Joint Propulsion Conf. and Exhibit (Salt Lake City, United States of America) (American Institute of Aeronautics and Astronautics)
- [98] Pivkina A, Ulyanova P, Frolov Y, Zavyalov S and Schoonman J 2004 Nanomaterials for heterogeneous combustion *Propellants Explos. Pyrotech.* **29** 39–48
- [99] Bockmon B, Pantoya M, Son S and Asay B 2003 Burn rate measurements of nanocomposite thermites 41st Aerospace Sciences Meeting and Exhibit 41st Aerospace Sciences Meeting and Exhibit (Reno, Nevada) (American Institute of Aeronautics and Astronautics)
- [100] Martirosyan K S and Lyshevski S E 2012 MEMS technology microthrusters and nanoenergetic materials for micropropulsion systems 2012 2nd Int. Conf. 'Methods and Systems of Navigation and Motion Control' (MSNMC) 2012 2nd Int. Conf. 'Methods and Systems of Navigation and Motion Control' (MSNMC) pp 133–6
- [101] Beck M W and Brown M E 1986 Modification of the burning rate of antimony/potassium permanganate pyrotechnic delay compositions *Combust. Flame* **66** 67–75
- [102] Puchades I, Hobosyan M, Fuller L F, Liu F, Thakur S, Martirosyan K S and Lyshevski S E 2014 MEMS microthrusters with nanoenergetic solid propellants 14th IEEE Int. Conf. on Nanotechnology 14th IEEE Int. Conf. on Nanotechnology pp 83–6
- [103] Zhou X, Ke X and Jiang W 2016 Aluminum/copper oxide nanostructured energetic materials prepared by solution chemistry and electrophoretic deposition *RSC Adv.* **6** 93863–6
- [104] Memon N K, McBain A W and Son S F 2016 Graphene oxide/ammonium perchlorate composite material for use in solid propellants *J. Propul. Power* **32** 682–6
- [105] Higa K 2007 Energetic nanocomposite lead-free electric primers *Journal of Propulsion and Power—J. Propul Power* **23** 722–7
- [106] Son S F 2003 Performance and characterization of nanoenergetic materials at los alamos *MRS Proc.* **800** AA5.2
- [107] Davila I 2017 *Biocidal Defeat Agents Produced by Silver-Iodine Nanoenergetic Gas Generators* The University of Texas Rio Grande Valley
- [108] Wang S, Schoenitz M and Dreizin E L 2016 Mechanically alloyed magnesium–boron–iodine composite powders *J. Mater. Sci.* **51** 3585–91
- [109] Patel V K, Saurav J R, Gangopadhyay K, Gangopadhyay S and Bhattacharya S 2015 Combustion characterization and modeling of novel nanoenergetic composites of $\text{Co}_3\text{O}_4/\text{nAl}$ *RSC Adv.* **5** 21471–9